Marine and Petroleum Geology 150 (2023) 106103

Contents lists available at ScienceDirect

Marine and Petroleum Geology

journal homepage: www.elsevier.com/locate/marpetgeo

Architectural complexities and morphological variations of the indus fan and its elements: Understanding of the turbidite system through seismic characterization

Ehsan ul Haq [a,b,*], Ji Youliang [a], Hadayat Ullah [b], Khurram Shahzad [c], Nisar Ahmed [d], Saad Ahmed Mashwani [b], Muhammad Zaheer [b]

[a] State Key Laboratory of Petroleum Resource and Prospecting, College of Geoscience, China University of Petroleum, Beijing, China
[b] Department of Earth & Environmental Sciences, Hazara University Mansehra, KPK, Pakistan
[c] Institut für Geologie, Universität Hamburg, Hamburg, Germany
[d] Department of Energy Resources, University of Stavanger, 4021, Stavanger, Norway

ARTICLE INFO

Keywords:
Indus fan
Submarine channels
Channel levee complex
Seismic facies
Mass-transport deposits

ABSTRACT

The investigations of the processes occurring in submarine fans improve the understanding of intricacies of deepwater turbidity system and their associated developed architectural elements. The seismic patterns and depositional geometries of the channel levee complexes of the Indus fan have been studied using 2D/3D seismic and well data. The Indus fan is the second largest submarine fan in the world, with a horizontal extent of some 1500 km and a thickness of approx. 9 km. The development source of the Indus fan is divided into two units primarily based on their stratigraphic architecture and depositional characteristics. Firstly, the Eocene-Oligocene to Miocene lower unit that is built of channel lobes, and regionally developed large mass-transport deposits including megaturbidites. The other unit is Miocene and the Quaternary upper part that constitute major channel levee complexes with minor intercalations of locally developed mass transport deposits. The former progressively increase in thickness and width upwards the Eocene-Oligocene to Quaternary. This gave rise to symmetrical and asymmetrical growth patterns as a result of multiple phases of erosion and deposition. Such an architecture is present at an extensive scale primarily in the Plio-Pleistocene channels where the vertical to lateral growth ratio is higher than the channels. A single episode of thick MTDs is recognized by seismic reflection geometries suggesting sea level fluctuations that occurred between the Eocene-Oligocene and the Miocene, and from the Pliocene and the Quaternary channels. Regional confinements drastically affected the development of the Indus fan from the Eocene-Oligocene to Miocene, diminishing from the Pliocene-Quaternary. Sediment zonation occurred owing to the presence of structural confinements that controlled the growth of channel levee complexes and in general the entire Indus fan. Our results based on seismic reflection data of channel levee complexes suggest that increasing but alternating sediment supply from Eocene till Plio-Pleistocene, assisted the active channels and levee growth. Continuous increase in turbidity current size and energy along with sedimentation rates modified (i.e., increased the channel aspect ratio) the channel architecture of the Indus Fan.

1. Introduction

The Indus fan is the second largest deep sedimentary body in the modern Indian ocean (also known as the Arabian sea) after its neighboring Bengal fan with a volume of 5.0×10^{6} km^3. The Indus fan stretches to 950 km in width and extends up to 1500 km in the Indian ocean in front of Indus delta (Clift et al., 2001; Clift and Gaedicke, 2002) (Fig. 1a). It includes the record of eroded sediments from the Himalayas, the Karakorum and the Hindu Kush mountain ranges since the middle Eocene (Clift and Gaedicke, 2002; Ehsan et al., 2016; Hussain et al., 2017). It is currently fed by a 185 km long submarine canyon with two paleo-canyons that are inactive presently (Kenyon et al., 1995; Prins and Postma, 2000) as shown in Fig. 1a. The Indus basin contains an ~10 km thick succession of the sediments from the Oligocene to Quaternary

* Corresponding author. State key laboratory of Petroleum resource and prospecting, College of Geoscience, China University of Petroleum, Beijing, China.
E-mail addresses: ehsaanarif@gmail.com (E. Haq), jiyouliang@cup.edu.cn (J. Youliang), hadayatkhan@hu.edu.pk (H. Ullah), khurram.shahzad@gmx.net (K. Shahzad), nisar.ahmed@uis.no (N. Ahmed), Saadmashwani@hu.edu.pk (S.A. Mashwani), mzaqau@gmail.com (M. Zaheer).

https://doi.org/10.1016/j.marpetgeo.2023.106103
Received 24 July 2022; Received in revised form 5 January 2023; Accepted 7 January 2023
Available online 10 January 2023

underlain by volcanic basement and carbonate platforms (Carmichael et al., 2009a; Gaedicke et al., 2002). With dominant control of the sea level changes, the turbidity currents are the major sediment source that developed the Indus fan (Naini and Kolla, 1982; Kolla and Coumes, 1983; McHargue and Webb, 1986; Kolla and Macurda, 1988).

Channel levee complexes (CLCs) and mass-transport deposits (MTDs) are the two important elements which are associated with the sedimentological processes of deepwater systems. Submarine channels are the conduits that transport sediments from canyon mouth onto the basin floor as illustrated in Fig. 2 (Mutti and Normark, 1987). Channel levee systems represent an erosional-depositional hierarchical style of the sedimentation of submarine fans like the Indus, the Bengal (Emmel and Curray, 1981), the Amazon (Damuth and Flood, 1985) and many others. Channel levee systems form a repository of coarse grained (channel floor) and fine grained (levees) sediments (Piper and Deptuck, 1997). Carmichael et al. (2009b) reported that the channels on the upper fan developed on the topographic lows on seafloor due to channel lateral accretions. It is now understood that the larger channels which are leveed constitute the smaller unleveed channels and their deposits representing different cycles of erosion and deposition (Gee et al., 2007; Hodgson et al., 2011; Mayall et al., 2006). This combination of channels and MTDs build deep sea fans through depositions of different sediment ratios (Bellwald et al., 2020; Damuth et al., 1988). The widespread MTDs are present in the Indus fan either overlying the CLCs predominantly of the Paleogene age or as channel fills, and consequentially interacting to develop a complex architecture of the Indus offshore.

The Indus fan has been investigated by the several authors during last three decades for its genesis, seismic geomorphology, and stratigraphic and depositional processes (Kolla and Coumes, 1985; McHargue and Webb, 1986; Clift et al., 2001; Gaedicke et al., 2002; Deptuck et al., 2003; Carmichael et al., 2009a). However, these studies exclusively describe the channel architecture on the Indus Fan with the aid of low-resolution and/or limited seismic reflection data. For example, previous studies such as McHargue (1991) have used 24-fold data and similarly, Kolla and Coumes (1985) have used single channel seismic data. In contrast to previous work, we used 160-fold multichannel seismic reflection data that inhabited the detailed analysis of architectural elements of the Indus fan. In addition, a recently available seismic reflection dataset from the offshore Indus Basin, Pakistan also provides an excellent opportunity to unravel the extensive and previously undocumented packages of MTDs and CLCs.

The objective of this investigation is to present the inception and genesis of the channel levee complexes and their corresponding series of the mass-transport deposits (MTDs), to explain their evolution and to discuss possible triggering mechanisms for these features across the continental slopes and the basin floor. In this study, 3D seismic data along with well logs measurements are used to identify the seismic patterns and depositional geometries of the channel levee complexes (CLCs) of the Indus fan. Further, to mark the channel's geometry and architecture, a range seismic attributes including trace envelop, horizon wavelet attribute, etc. Are used. This work is novel and the investigations of the processes occurring in submarine fans helps to

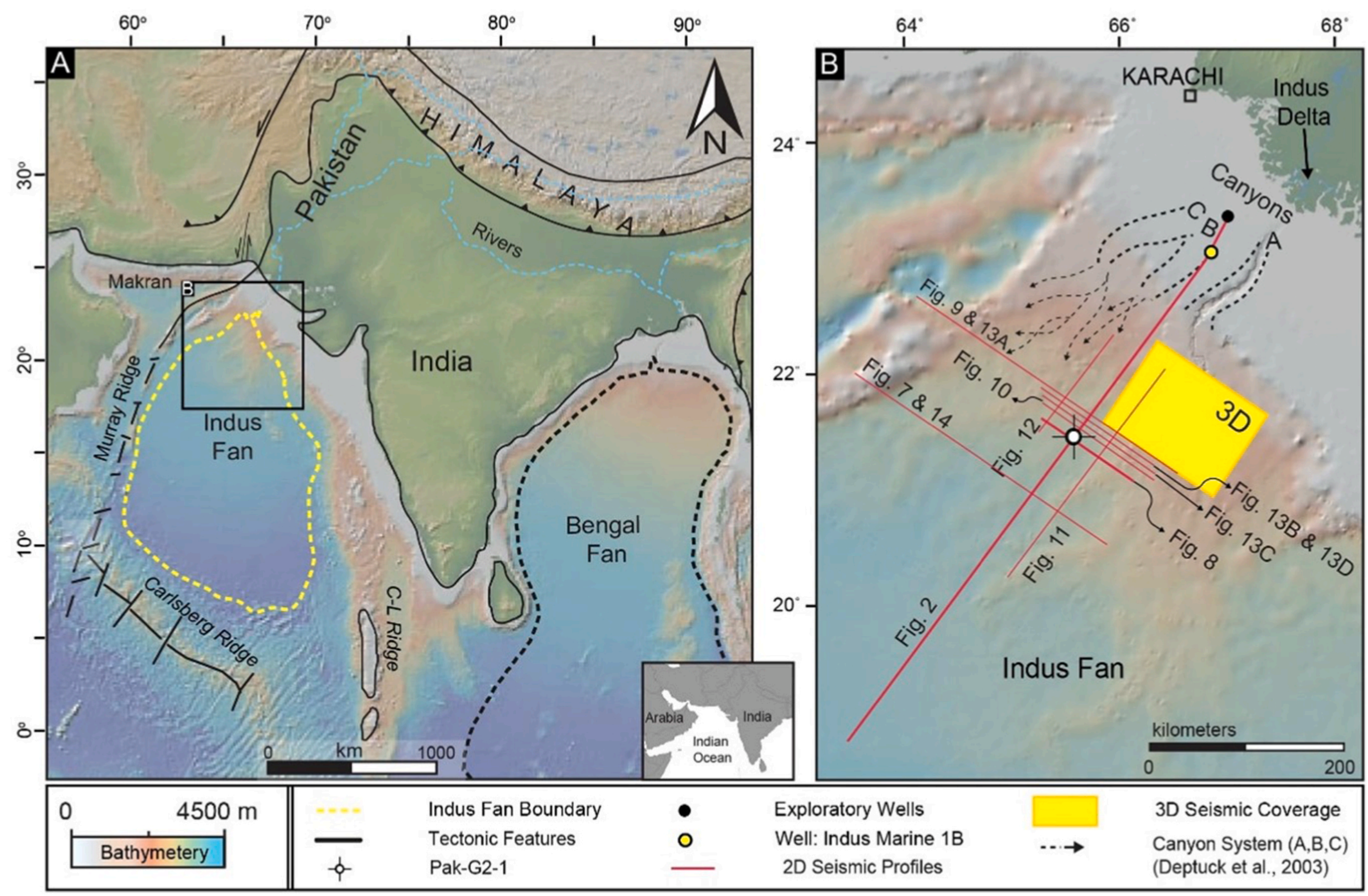

Fig. 1A. A: Location map of the Indus fan and the boundary of the Indus fan, its distributions, and adjacent morphological features are also marked on the map. Bengal fan is also shown on the right-hand side of the map. B: 2D seismic data transects are shown on the map that outlines the extent of the dataset along with the figure numbers. 3D data set is highlighted in yellow color. Three canyons "A", "B" and "C" are shown on the map that acted as the source of sediment supply to the fan. wells Pak G2-1, Pakcan-1 and Indus Marine 1B is highlighted on NE-SW trending seismic line. Color legend is visible displayed for topography and relief. Source: Geo-map app, **1b.** Showing the synthetic seismogram generated by convolving the seismic wavelet (Ormsby) with the subsurface reflectivity series (RC), **1c.** The synthetic seismogram is plotted along with seismic data at the well (Pakcan-1 01) location and it very well correlated with the seismic profile.

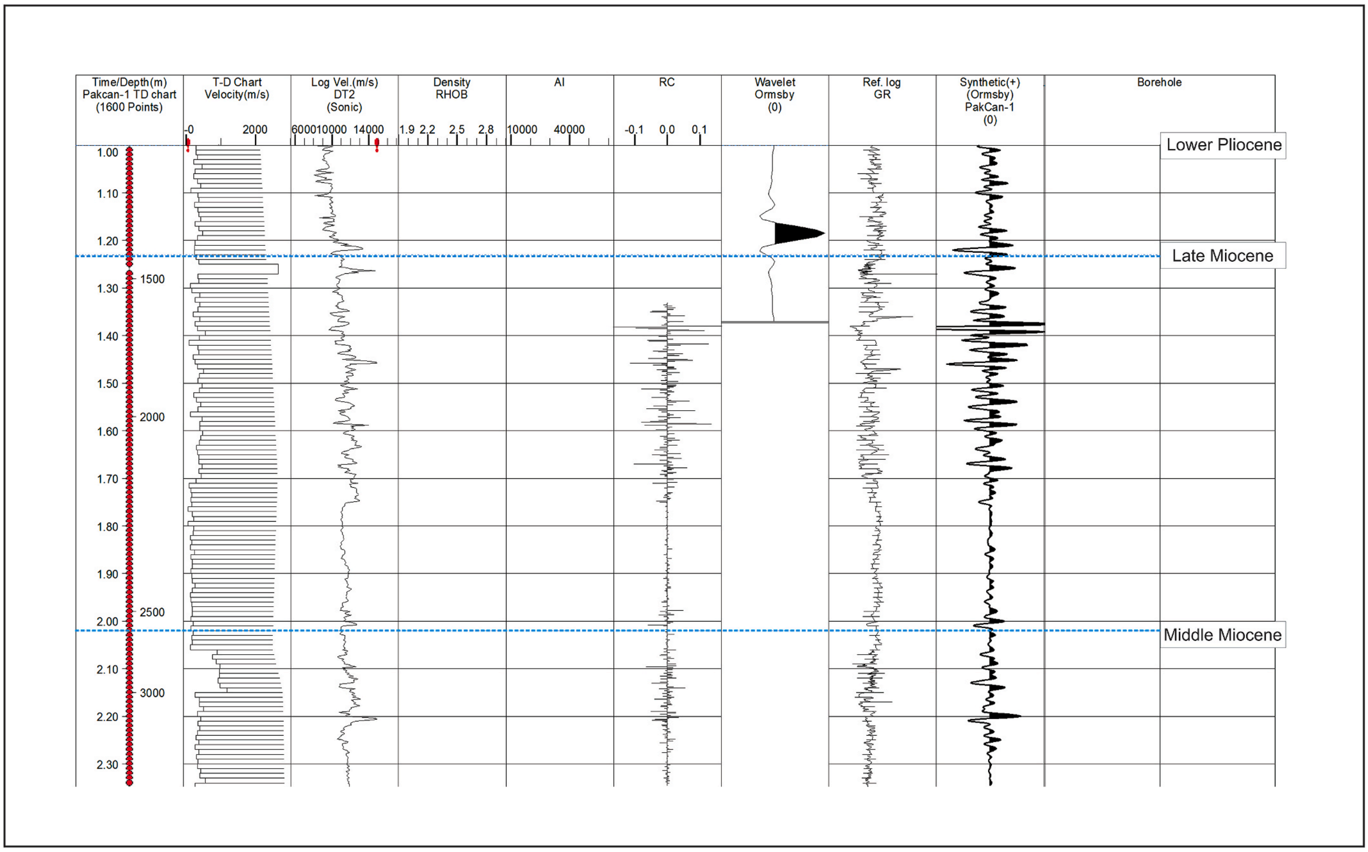

Fig. 1A. (*continued*).

improve the understanding of intricacies of deepwater turbidity currents and their associated geometrical elements.

In the following, we first review the geological setting of the study area followed by the data used and the methodology of the research work. Then, we illustrate the results of our interpretation carried out by following the research approach defined in the methodology section. At the end, a comprehensive discussion based on the results has been made. envelope modulated phase.

2. Geological setting

The development of the offshore Indus Basin is associated with the separation of the Indian Plate from the African Plate in the Late Jurassic (ca.150 Ma) (Gombos et al., 1995; Gaedicke et al., 2002; Hussain and Ahmed, 2018). Following the separation of the Indian Plate from the Madagascar in the Late Cretaceous (ca, 90 Ma), its northward drift and collision with the Eurasian Plate occurred during the Middle Eocene resulting to the rise of the Himalayan mountain ranges that initiated the north-south drainage basin system. After the collision, deposition of the eroded sediments in the foreland basin occurred along the passive continental margin known as the offshore Indus Basin, Pakistan at least since the Eocene (Curray, 1994; Ahmed et al., 2020; Ghazi et al., 2020).

The study area covers the proximal setting of the Indus fan, which constitutes the northwestern Indian continental margin, in the offshore Indus basin (Fig. 1a). The Indus fan is a river fed submarine fan system developing at the triple junction bounded by multiple geomorphologic features. In the west, the Indus fan is bounded by the Chagos-Laccadive Ridge while the Carlsberg Ridge and the Owen-Murray Ridge borders the fan from the south and northwest to the west direction respectively (Fig. 1a).

The early development of the Indus fan is evident from the presence of the middle Miocene sandstone in the distal part of the Indus fan which is originated from the Indus suture zone and were transported by a proto Indus River system (Clift et al., 2001). Along the continental slope, in the shelf-slope areas, three channel-canyons feeding systems have been identified that served as the conduit for sediment transport from river mouth to the deep water submarine fan system (Deptuck et al., 2003; Prins, 1999).

3. Dataset and methodology

3.1. Seismic and well logs data

This research work uses datasets comprise of 2D and 3D seismic and borehole wireline logs acquired in the offshore Indus Basin, Pakistan. Seismic surveys were acquired in 2001 and 2002 at water depth of ~2700 m covering an area from shelf to the basin region (Fig. 1a). The standard seismic data includes 2D and a 3D pre-stack time migrated (PSTM) volumes. The 2D time migrated seismic surveys covering an area of 75,000 km^2 with a grid spacing of 5 × 5 km. The record length of 2D seismic data is around 12 s which is sampled at the interval of 2 ms. Seismic data has zero phase and displayed in the normal polarity (Brown, 2011). The polarity behavior of the data is defined by black and red reflections describing positive acoustic impedance and negative acoustic impedance respectively. The vertical resolution of seismic data is approximately 25 m and has dominant frequency of 45 Hz.

The well logs data from three different wells, drilled in the study area is used for well to seismic stratigraphic correlation. Only Packcan-1 well has check shot data available for the current work, whereas only well log data is available for the Indus marine 1B and Pak G21 wells. Therefore, a synthetic seismogram is generated by using the time-depth (TD) chart of the Packcan-1 well and used for the horizon identification (Akram et al, 2020). The synthetic seismogram generated from the Packcan-1 well TD chart is shown in Fig. 1b and synthetic overlapping with real seismic

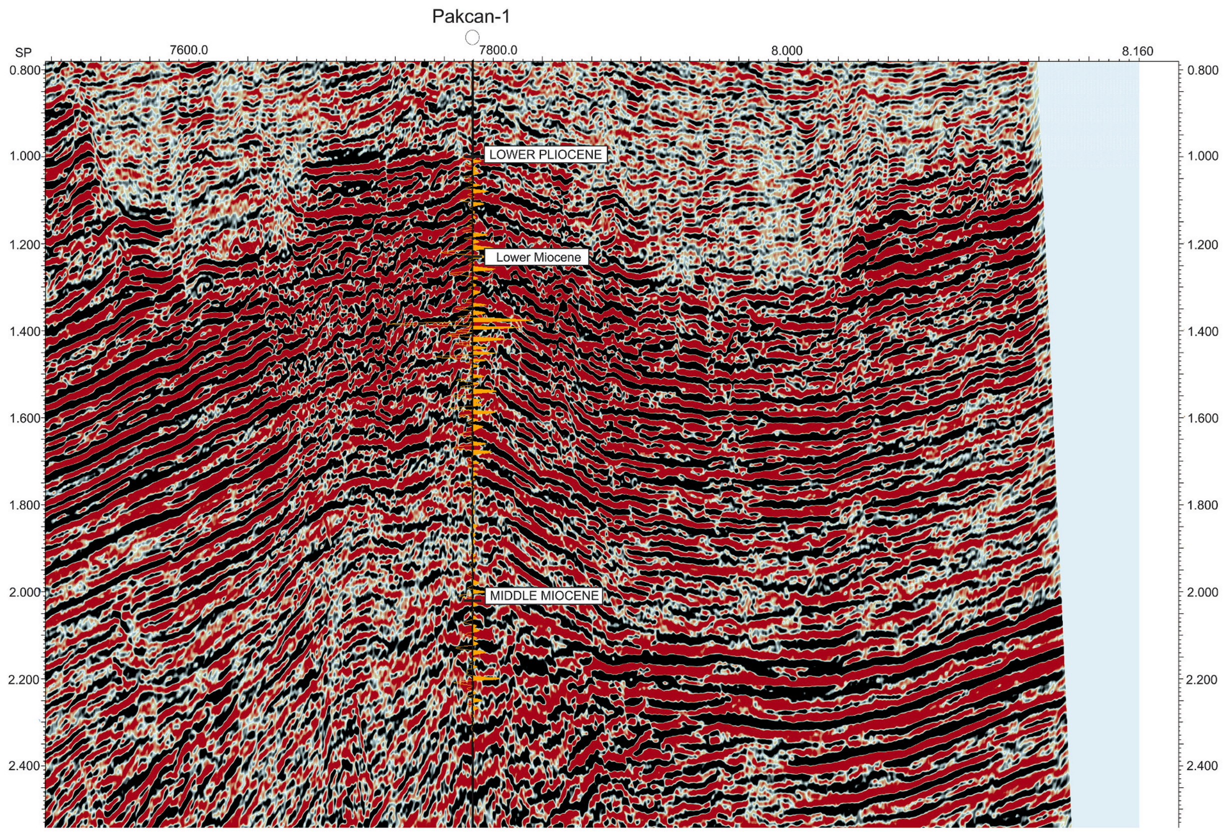

Fig. 1A. (*continued*).

data is displayed in Fig. 1c. The synthetic seismogram is showing good overlapping with seismic section. The available well log data for this study contains standard wireline logs suits e.g., gamma ray (GR), sonic time (DT), density, neutron porosity and other wireline logs.

The methodology workflow started with the identification of geological horizons (e.g., from Eocene to Pleistocene) for the geological age correlation of seismic events using available wireline logs and seismic data (Vail et al, 1977). The well data used in this study are the Indus Marine 1B, Pakcan-1 and Pak G2-1 (Figs. 2 and 3). The Indus Marine 1B and the Pakcan-1 are drilled on the present-day shelf whereas the Pak G2-1 is located on the continental rise. Check shot data provides the well to seismic correlation for geological age control. The Indus Marine 1B and Pakcan-1 are drilled down to the Miocene section of the shelf while the Pak G2-1 well is drilled to a depth of over 4500 m that penetrates the carbonate platform (Fig. 3) (Shahzad et al., 2019). The core data and well cuttings are not available for these wells and therefore, the detailed identification of the mineralogical composition of lithologies not possible.

3.2. Research approach

For seismic stratigraphic interpretation, we followed the approach defined by Mitchum et al. (1977). Based on well-to-seismic correlation, the Cenozoic succession can be divided into two major stratigraphic units i.e., the Eocene-Oligocene to the Miocene and Plio-Pleistocene to the Recent (Holocene) epochs.

A hierarchical approach (Gardner et al., 2003; Abreu et al., 2003; Campion et al., 2000; Mayall et al., 2006) is adopted to characterize the submarine channel systems: where larger erosional features are packed by turbidite beds which stack upward to form channel fills located inside the channel form. Channel basal erosive and bounding surfaces along with confining levees are investigated for their geometry downslope from base to top of the Indus fan. The scale and stratigraphic distributions of geomorphic features were displayed using 2D and 3D seismic data. CLCs are analyzed for their depositional style and architecture for each unit. Seismic attributes improve the visualization of CLCs in a two-dimensional view that augments the recognition of small-scale depositional features. Time and horizon slice attributes were generated to image the planform geometry of channels and to envisage their pattern and depositional nature. For this work, we have used Ormsby wavelet which provides the most redefined spectrum and therefore, is an appropriate choice for seismic reflection data analysis. Ormsby wavelet is computed from a trapezoidal frequency spectrum with parameters are frequency F1 05 Hz, frequency F1 10 Hz, frequency F1 45 Hz and frequency F1 60 Hz. The root mean square (RMS) seismic attribute, estimate the square root of amplitudes to describe the internal architecture of the channel levee complexes that improve the understanding of three-dimensional channel models.

The stratigraphic and structural interpretation of the seismic dataset is carried out by using the Petrel and the Kingdom suits. The stratigraphy was extrapolated to the seismic data from the wells data i.e., the Indus marine 1A and the Indus Marine 1B, located on the continental shelf. The well Pak-G2-1 and the stratigraphic model described by Carmichael et al. (2009a) was utlized for deep-water stratigraphic control. This

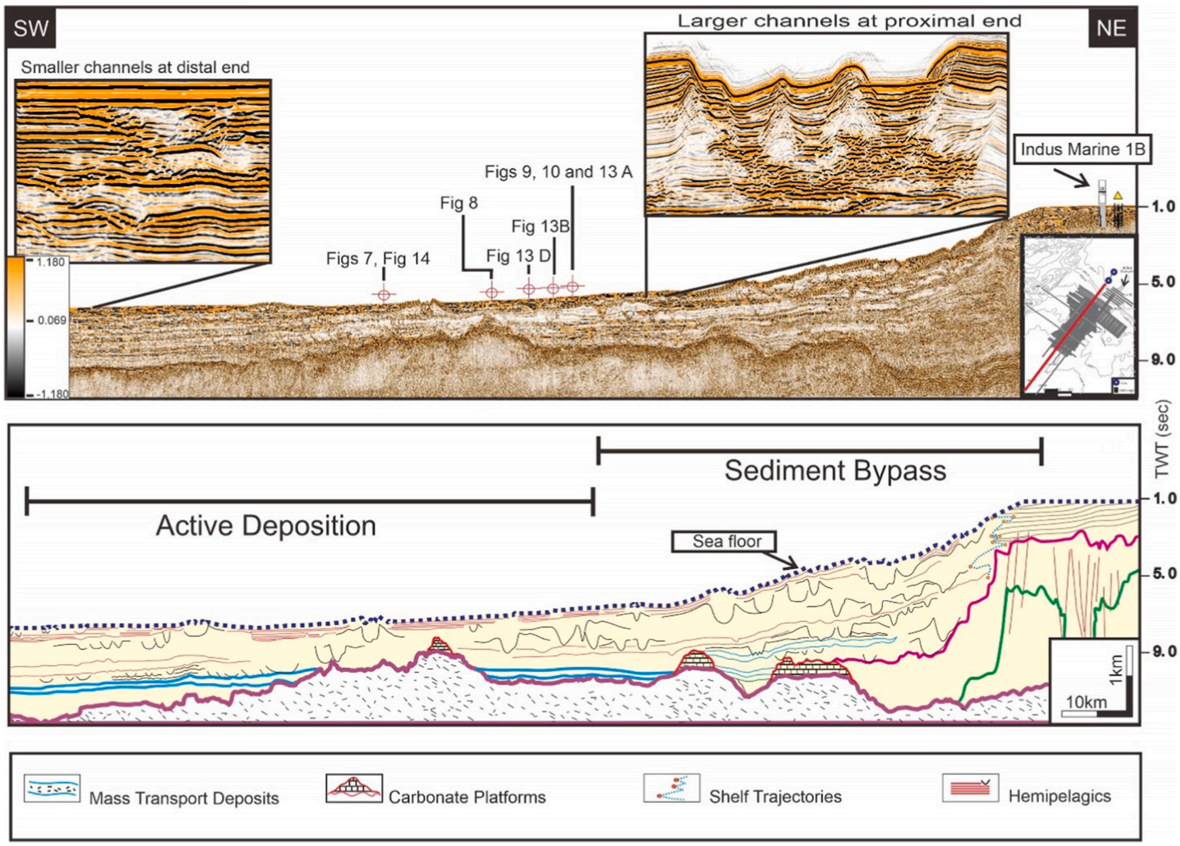

Fig. 2. A 2D seismic profile along the Indus fan, and oriented in the NE-SW direction. It shows major elements of the Indus offshore basin from the volcanic basement to sea floor (bottom to top). Volcanic basements are overlain by carbonate platforms and thick succession of the Indus fan. Carbonate Mounds: Color interpretation can be described as, purple outline color with white fill represents basement; green and purple solid lines represent paleo-shelf; black wavy lines mark the erosional surfaces of channels; blue dotted line represents the sea floor and the extent of interpreted seismic line. Inset images show the varying channel sizes on the proximal and distal portions of the fan (the area overlain by base map is out of study zone).

provides a control of the chronostratigraphic framework for the Indus fan succession and older sedimentary deposits. A mean seismic velocity of 2500 m/s is used for the seismic interpretation gridding and subsurface depth mapping of the Plio-Pleistocene age interval.

4. Results and observations

4.1. Seismic stratigraphy

4.1.1. Detailed seismic facies of architectural elements

The Upper Indus fan shows a variety of seismic facies with assortment of lithological and depositional features e.g., unidirectionally migrating channels are shown in Table 1. These seismic facies and morphological features are based on their geometries, texture, and characteristics from seismic profiles (Table 2) and can be interpreted for their possible depositional environments through their seismic character (Schwenk and Spiess, 2009; Mayall et al., 2006; Deptuck et al., 2003; Mutti and Normark, 1987; Normark et al., 1980; Normark, 1978).

4.1.2. 3D seismic morphology of channels

Time slices and horizon slices of three CLCs of Plio-Pleistocene age display the planform morphology of the channel belts and are shown in Figs. 4 and 5. The time slice is generated by using trace envelope attribute at two-way-travel time (TWT) of 2.44 s for the two channels belts which shows low to moderate sinuosity (Fig. 4). Trace envelope attribute also known as reflection strength exhibits strong acoustic seismic events. This attribute is computed from the complex seismic trace (analytical and quadratic trace) and is utilized to identify the major seismic features e.g., impedance, tuning effects, deposition environment, lithological variations, sequence boundaries, gas accumulation zones, unconformities, and fault identifications etc. The envelope attribute describes the instantaneous seismic energy of the reflected even and is directly related to its magnitude of the reflection amplitude. The benefit of using the envelop attribute over the real trace values is that it is not dependent on the seismic data polarity and the phase of the seismic data.

The second-order differentiation of the trace envelop provides the measure of envelope peak sharpness and presents all the peaks of the envelope, which refers to all the reflecting boundaries observable inside frequency bandwidth of seismic data. Further, the higher derivative displays sharpness of seismic events, changes of lithology, depositional environment variations, etc.

Mathematically, the second derivative equation can be defined as

$$\frac{d^2\,E(t)}{dt^2} = E(t) * \;diff(t) * diff(t)$$

here, *E(t)* indicates the trace envelop, *diff(t)* refers the differential operator, and the symbol asterisk ($*$) is for convolution.

The channel belt displayed in yellow color represent of relatively low sinuosity as compared to the channel belt in red. An arcuate feature in the middle of the red channel belt suggests a possible channel avulsion of the green channel belt (Fig. 4). Adjacent to avulsion point a zone of neck cut off is marked in pink color that signifies the straightening of the channel near a sharp meander bend. An older channel on the right side of the red channel develops a wider channel belt which illustrates higher turbidity flows and swing of the channel thalweg.

A horizon wavelet attribute is utilized to generate a horizon slice (at TWT of 2.74 s from sea floor) reveals several distinctive features (Fig. 5).

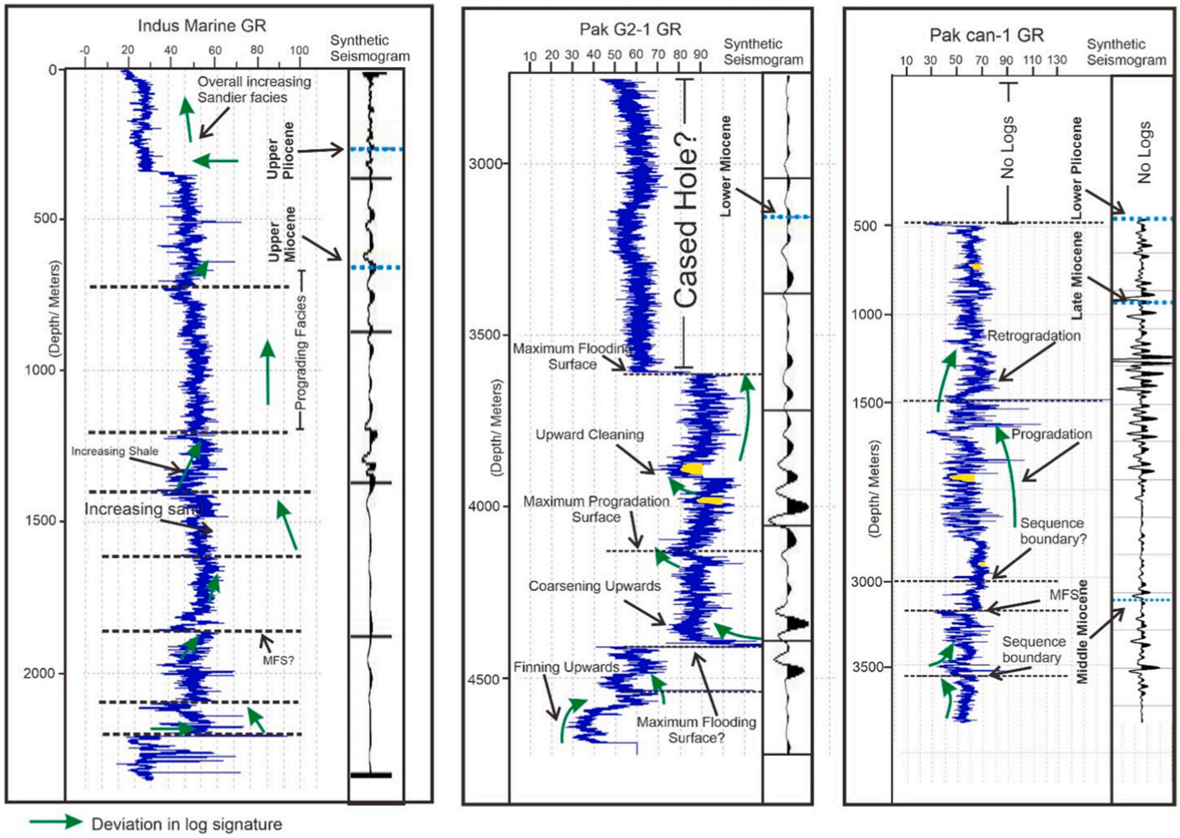

Fig. 3. Gamma ray logs of all three wells named as the Indus Marine 1B, Pak G2-1 and Pakcan-1 are displayed. The well logs are generally used in the study for the purpose of age correlation. Log responses are interpreted for the lithology that aided in outlining the main time surfaces. Color interpretation: green arrows mark the deviation on the logs in response to lithology; black dotted lines mark the points of interpreted significant time surfaces.

Table 1
Shows the dimensions of outer levees of unidirectional channels i.e., both unidirectionally migrating major channels (UDMa) and unidirectionally migrating minor channels (UDMi).

Channel Type	Max. Thickness outer bank levee	Max. Thickness Inner bank levee	Avg. outer levee	Avg. inner levee	Age
Levee extension (km) (UDMa)	15.981	21.263	11.87	13.96	Plio-Pleistocene
Levee thickness (m) (UDMa)	437.5	700	283.92	441.87	Plio-Pleistocene
Levee extension (km) (UDMi)	11.65	16.45	8.95	7.12	Pleistocene
Levee thickness (m) (UDMi)	300	420	230	257	Pleistocene

In the horizon attribute, amplitude extraction is applied just as characteristic of the horizon. This attribute can be extracted by applying few steps in a Petrol software package e.g., select a horizon of interest, define a volume to extract, adjust the minimum and maximum time window. The planform section (defined by red color) of the Pliocene age channel suggests low sinuosity of the channel belt. On the contrary, LAPs and thick levee (Fig. 5, point 1) in the eastern corner (yellow, semi-circle), suggest that channel thalweg had higher sinuosity inside a channel belt. Channel may also have gone through avulsion in the later stage of evolution (Fig. 5, point 3). Sediment waves (Fig. 5, point 5) are deposited (as discussed earlier) near the channel belt reminiscent of flow stripping. In the upper right corner of the profile two channel forms merge downslope. In the south-west corner of the profile another wider (unmarked) channel belt is present, (not described due to data constraints).

Seismic envelope modulation attribute maps generated at TWTs of 29.3 s, 2.90 s, 2.73 s, and 2.70 s marked as 1, 2, 3 and 4 respectively in Fig. 6 display the channel growth and its characteristic sinuosity. The envelope modulation attribute describes the slow amplitude modulations in a seismic signal. It also defines the distribution of energy in seismic reflection coefficient fluctuation across specified frequencies. The envelop for the n signals ($e_i[n]$) is denoted by the convolution of analytical signal and impulse response. The variations in the characteristic sinuosity from older to younger channels are marked by yellow dotted lines. The older buried channels increase in sinuosity with increasing meander bend and channel width as shown in Fig. 6 (profiles 3 and 4). Channels are bounded by high amplitude reflections that also increase in extent from older to younger channels. At TWT of 2.73 s, channels become relatively straight compared to its older underlying channels followed by an increase in width at 2.70 s illustrated in Fig. 6 (profiles 1 and 2). The outer bends show lack of high amplitude reflections contrary to the older channels.

4.2. *Channel architectural elements and morphological variations*

4.2.1. *Eocene to miocene channel levee complexes*

The 2D seismic data show the channel complexities from the Eocene to the Miocene of the Upper Indus fan. (Figs. 7–9). Channels are confined as well as unconfined erosionally with well-developed outer levees.

Table 2
Assessment of seismic facies constituting the Indus fan from volcanic basement of cretaceous age to channel levee complexes of Indus fan overlain by hemipelagic deposits during the sea level high stand.

Seismic Framework	Seismic Expression	Depositional Characteristics (Seismic)	Interpretation
Seismic Facies 1 Pleistocene-Quaternary Channel with Hemipelagic Succession on top	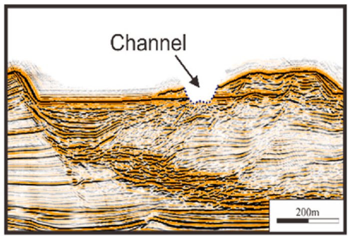	A recent channel incised the hemipelagic succession draping the Indus Fan sediments. The unfilled channel is suggestive of early phase of development	Even during high stand sea level conditions minor channel incisions occur that supply the sediments to distal portion of the fan.
Seismic Facies 2 Sediment waves on Pleistocene Channel Levees overlain by Hemipelagic Drapes	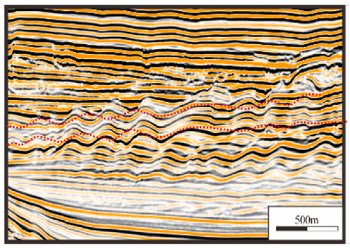	Sediment waves with parallel to subparallel crests. Pleistocene channels are flanked by Levees with abundant sediment waves in Indus Fan	Flow stripping of turbidity currents modify the architecture of levees and develop sediment waves
Seismic Facies 3 Frontal Splay bounded on top and bottom by Channel levees	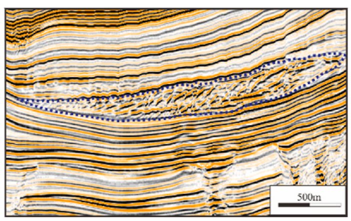	Concave up features with dipping minor seismic reflection developed on the Indus fan adjacent to channels	Frontal Splay mark the unconfined flow of turbidity currents that developed as the channel flows unconfined downslope and deposit the sediments load
Seismic Facies 4 Channelized Lobe with minor distributary Channels	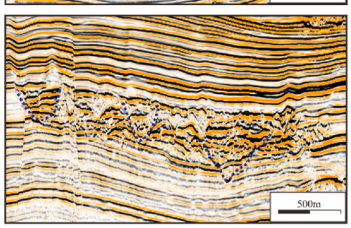	Channel Lobe incised by successive distributary channels bounded on top and below by cyclic deposits	Following the deposition of channel lobe, younger successive currents channelize the lobes.
Seismic Facies 5 Channel Levee Complex with predominant lateral migration and overlain by Pleistocene Channel Levee Complexes	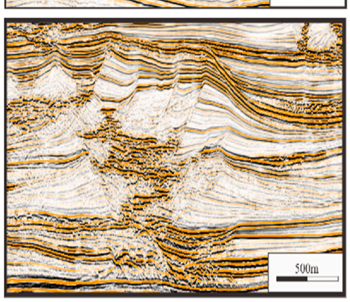	Indus Fan is dominated by major Channel Complexes that increase in width and thickness from Eocene-Oligocene to Plio-Pleistocene	Multiple cycles of cut and fill followed by channel abandon stage and reactivation respectively, creates the complex features
Seismic Facies 6 Megaturbidites of Indus Fan with minor Channel Incisions (bottom to top)	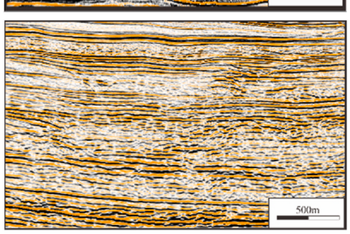	Thick Succession of megaturbidites lie underneath the Indus Fan sediments. These megaturbidites are incised by the channels.	According to (Bourget et al., 2013) megaturbidites of Indus fan are of local origin.
Seismic Facies 7 Volcanic Basement underlying Indus Fan sediments	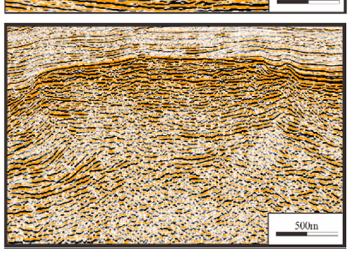	Volcanic basement underlies the Indus Fan deposits. Volcanic highs and carbonate platforms provide confinements that restricts the growth of Indus fan	Major confinements created as Indian plate moved over a reunion hotspot while drifting northward. These confinements create sediment portioning in Indus fan.

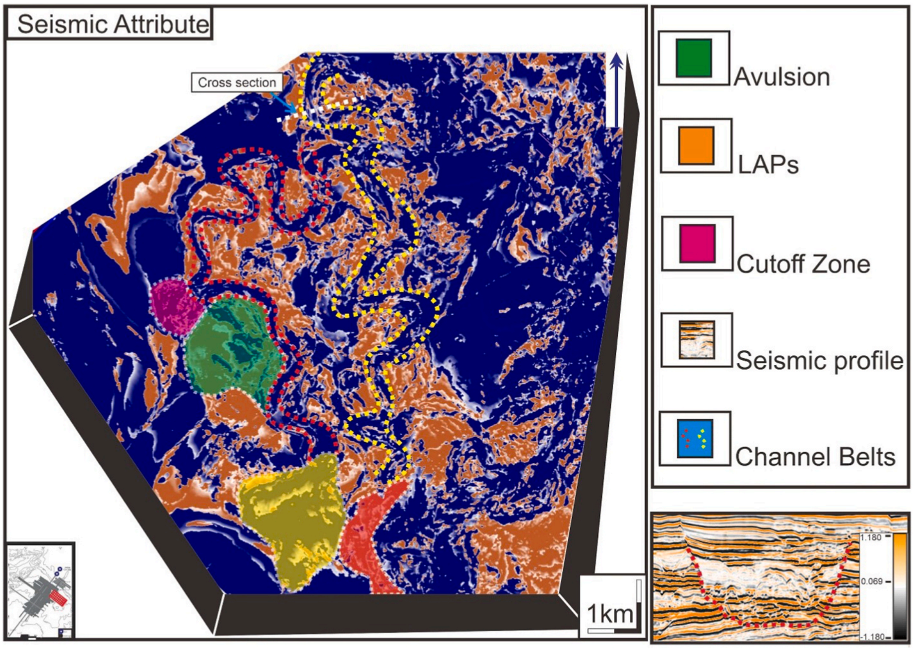

Fig. 4. Trace envelope modulated seismic attribute map of seismic profile displayed. Time slice (trace envelop) map generated at 2.4 s below the sea floor for a Pliocene age channel. The younger channel in yellow boundaries (dotted lines) vary in width downslope whereas the older channel in red dotted lined maintains the width because of lack of lateral migration and bank erosion. Various colors i.e., blue curve represents zone of cutoff: green curve is the zone of avulsion: lateral accretionary packages (LAPs) are also visible in the map. Brown and white color reflections on seismic profile represent amplitude variations. Red dotted line on the seismic profile marks the basal erosive surface of the channel.

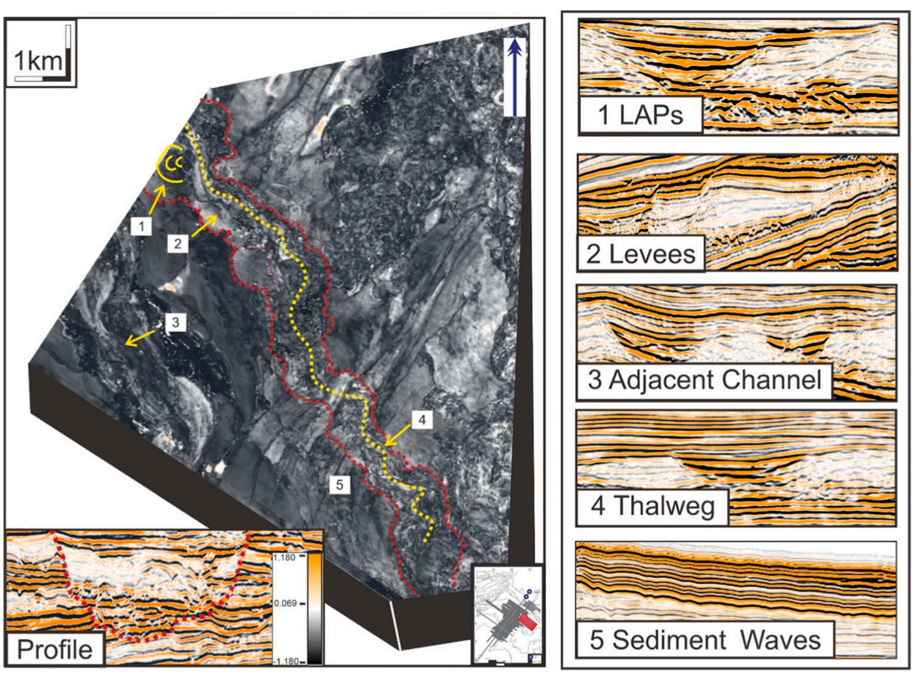

Fig. 5. Horizon wavelet attribute map generated from 3D seismic data to identify the apparent behavior of the channel. Submarine channel belt boundary is delineated in red. 1) Lateral accretionary packages: 2) channel levee buildup: 3) Adjacent channel: 4) thalweg: 5) sediment waves. Color interpretation: Thalweg is represented by yellow dotted line; Brown, black and white color reflections on seismic profile represent amplitude variations (polarity). Red dotted line on the seismic profile marks the basal erosive surface of the channel.

Erosion and deposition cycles are infrequent because of low and consistent sedimentation that is indicated through small channel sizes with no resolvable inner levees. Channels have been developed in mega turbidites of the Indus fan with interspersed MTDs, which are deposited above the volcanic basement and carbonate platform (Figs. 7 and 8). The depositional pattern inside the channels from the Eocene to the Miocene part of the fan does not evince an organized pattern because of lower intensity of turbidity flows.

4.2.2. Plio-Pleistocene to quaternary channel levee complexes

The Plio-Pleistocene channels of the Indus fan typically show higher incision and aggradation channel levee complexes. The channels are as wide as 12 km whereas the levees thickness reach up to 450 m (Figs. 7–9). The channels show a significantly similar architectural style (may be a different pattern) that comprises of lateral to vertical channel fill bounded by thick inner levees. Various authors (Burbank and Beck, 1991; Metivier, 1999; Clift et al., 2002) reported the peak sedimentation between 16 and 2 Ma i.e. (Miocene to Pleistocene). The amalgamation of the three different channel levee complexes is identified and illustrated (Fig. 9). Each channel shows overall decrease in width and thickness from bottom to top. The nature of basal erosive surface is apparently similar constituting terrace like features overlain by high amplitude continuous to discontinuous reflection packages that have been introduced in other submarine fan systems as well (Flood et al., 1991; Hübscher et al., 1997). The central profile shows a low amplitude channel fill at the base that continues laterally towards the direction of

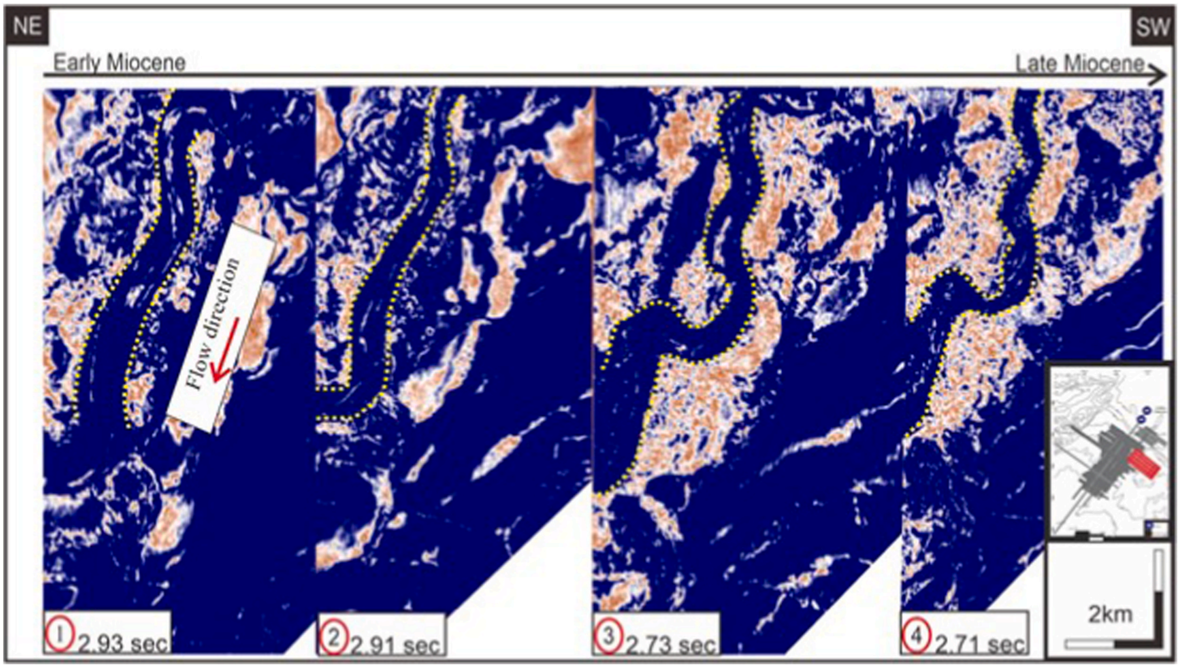

Fig. 6. Envelope modulated phase attributes for channels at 2.93, 2.90, 2.73 and 2.70 s from the early Miocene to the late Miocene. Channel marked in 3 and 4 widened over the course of development and an increase in meander occurred followed by abandonment and development of a younger and straighter channel marked in 1 and 2 displaying channel widening due to bank erosion. Channels are bounded by high amplitude reflections developed due to stripping and overspilling of overfit channel currents. Turbidity current flow direction is marked by an arrow. Color interpretation: brown color shade adjacent to channel margin represents levees and over bank deposits.

migration of the channel (Fig. 9). Although the top cross-section may predict a thinning and decrease in the width of the channel but CLCs in the Indus fan progressively grow to be deeper and wider towards the sea floor. Younger channels show high sinuosity in the Indus fan both the individual channels and the incisions near the abandonment phase of the channel (Fig. 9). Quaternary channel near the sea floor is erosional confined, devoid of the fill and lack the seismically resolvable inner or outer levees (Table 2, facie 1).

4.2.3. Architecture of the levees

The outer levees in the Indus fan are well developed in the Eocene-Oligocene to Recent channel levee complexes. The thick outer levees are dipping at high angle near the erosive surface of the channel gradually decreasing in dimensions (Figs. 7–9). From the Miocene to recent, levees are highly complex and thick unlike the levee build up before the Miocene. Multiple channel erosion and deposition cycle augmented the growth of outer levees as well as inner levees (Figs. 2 and 7–12). Undulating features on the backslope of the channel levees are fine-grained sediments referred to as sediment waves (Table 2; facies 2, Figs. 8 and 10) (Normark et al., 1980). Here, on the Indus fan, the features are well developed on the levee backslope with wavelength ranging from 122 m to 1473 m and a height of ~10 m–60 m (Fig. 10).

The analytical calculations of at least 14 unidirectionally migrating channel levee complexes (i.e., the aspect ratio of the laterally migrating channels) show that the average thickness of the outer levee is ~500 m (averaged) that is almost double in thickness compared to the levee on the inner bend which is 300 m (averaged) (or in the direction of migration) (Table 2). Levee architecture reflects the degree of flow confinement (Kane et al., 2008; Peakall and Sumner, 2015). Abrupt and persistent laterally migrating channels show decreasing confinement towards the abandonment of the channel (Figs. 10 and 12). Contrary to the unidirectionally migrating channels, the vertically aggrading confined channel levee complexes show symmetrical channel levee growth (Fig. 6).

4.3. Unidirectionally migrating channels

Migration of channels in the Indus fan is approximated by a predominant unidirectional migration of channels and contrasting levee build-up which is not unique to a few CLCs. Two different types of unidirectionally migrating channels are observed in the Indus fan, for example, unidirectional migrating channels major (UDMa) and unidirectional migrating channel minor (UDMi). Channels are categorized on the basis of channel levee dimensions (channel size and thickness to width ratio) and abandonment to reactivation cycles. Three distinct phases of channel growth are observed UDMa (Fig. 10). The initial phase of the channel builds up is marked by high amplitude reflection (HAR) packages at the base of the channel with substantial vertical growth. The angle trajectories suggest that the vertical growth of the channel is represented by higher angles of 72^0 (Fig. 12**).** The second phase of the channel development indicates the predominant lateral migration of the channels. The first part of second phase resembles the growth of initial phase of the CLS except for development of higher lateral migration (Figs. 10–12). Lateral migration of the channel is represented by lower angles 14^0 to 30^0 (Fig. 12). Linear, continuous HAR reflect the migration that affects the development of thick outer levees opposite to direction of migration. High amplitude reflection packages are bordered by inner levees that developed opposite to the direction of migration. The similar features on the Bengal and the Indus fans were observed in their study (McHargue, 1991; Hübscher et al., 1997; von Rad and Tahir, 1997). The third phase of CLS build-up is marked by abandonment stage of the channel levee system. Alternating high and low amplitude parallel to subparallel reflections mark the abandonment stage of the channel build up (Fig. 12).

UDMi channels display a hockey stick shape geometry also associated with laterally migrating channels (Fig. 11). This geometry is mainly present in the Pleistocene channels. As a result of lateral migration of the channel when coupled with aggradation owing to a limited and decreasing confinement hockey stick shape features development. UDMi channel fill is a combination of high amplitude discontinuous reflections

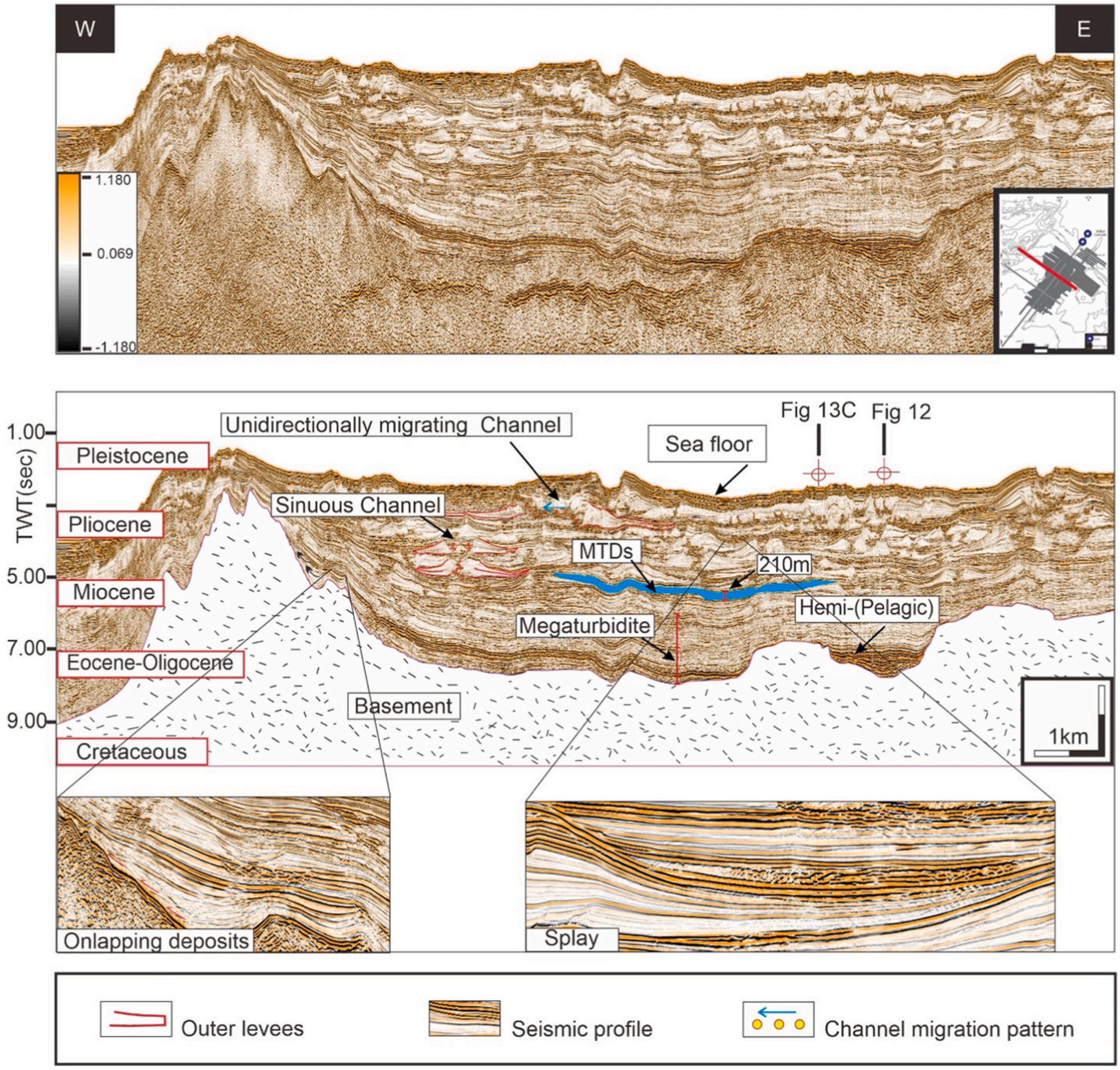

Fig. 7. Age distribution of the Indus fan deposition from the Eocene-Oligocene to the Pliocene. Channel size increase abruptly from bottom to top of the Indus fan. Volcanic basement provides the confinement which hindered the lateral growth of the Indus fan and created the sub-basins that accommodated the thick succession of megaturbidites. Color interpretation: white color fill represents the volcanic basement; brown and white color reflections on zoomed in seismic profile represent amplitude variation. Inset images show different features observed on the Indus fan.

deposited inside a narrow conduit bounded by outer levees and constrained by inner levee on one side. UDMi show lateral to vertical channel fill deposits with a vertical aggrading component as the channel maintains the equilibrium profile that terminates with the deposition of finer sediments causing the abandonment phase of the channel development (Fig. 11). UDMi channel are smaller compared to UDMa channels in both thickness and width with a strong contrast in the levee geometry. UDMi channels unlike UDMa channels have well developed outer levees (Table 1). Levees in the direction of migration are steeply dipping contrary to these gently dipping levees that are deposited opposite to migration direction. Such channel fills preserve the record of flow variations and the nature of highly confined turbidity currents.

Migration of single channel over time create dipping reflectors either parallel or towards the channel axis commonly referred to as lateral accretionary deposits (Fig. 13). Reflection pattern may vary from unidirectional dipping reflections to bidirectional dipping reflections. It is important to note that Lateral Accretionary Packages (LAPs) may be parallel to direction of migration with up dip and down dip component of migration (Fig. 13).

4.4. Variations in thickness of indus fan

Based on the NE-SW and E-W oriented seismic lines, investigations and calculations delineate the structural highs and carbonate platforms on the Indus fan that influenced the deposition in the turbidite system (Figs. 2, 8 and 14). Confinement here are provided by volcanic basements and carbonate platforms that developed on the subsurface highs.

Pelagic and hemipelagic deposits have developed between these confinements whereas slope failure deposits have also been distributed up and down slope these features. The thickness of the fan significantly varies upslope and downslope of the confinements. Immediately in the region downslope of the shelf break the fan thickness reach to 5.6 km with an average velocity of 2500 m/s (Fig. 2). This negative relief is created by the topographical high and the carbonate platform developed above it. Fan thickness decreases abruptly to ~4 km on top of confinement (Fig. 2). Thickness of the fan again increases to 4.8 km after the confinement but the second confinement on the slope traps the flow of sediments thus further reducing the thickness of the turbidite system to 2.4 km. The hindrance in fan growth continues downslope until the fan

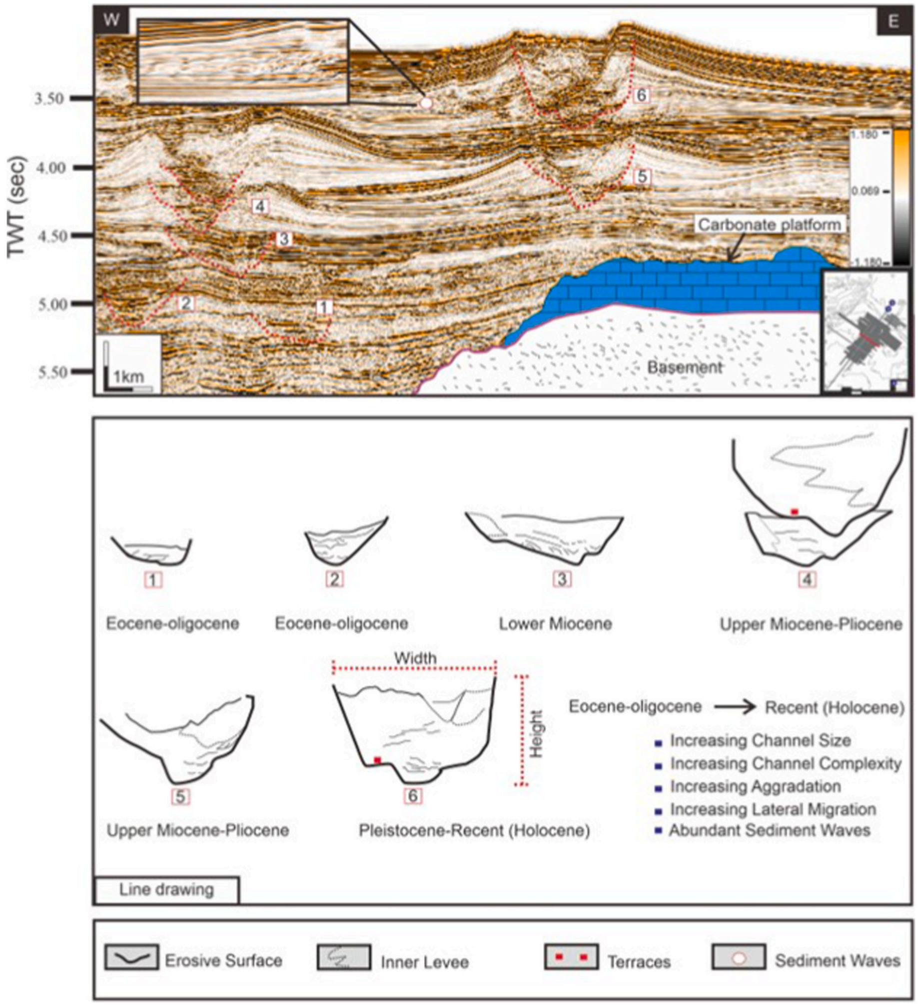

Fig. 8. From top to bottom, the upper seismic section highlighting the channel boundaries (basal erosive surfaces). Lower figure shows an increase in channel dimensions is observed from the Eocene-Oligocene to the Quaternary which is epitome of increasing sedimentation. Color interpretation: white color at the bottom represents volcanic basement; blue fill represents the carbonate platform. Brown, black, and white colors reflections on seismic profile represent the amplitude variations. Inset image show the sediment waves, the features that are rarely observed on channels other than the Pleistocene age.

displays parallel to subparallel facies in the study area.

Murray ridge of Cretaceous age acts as confinement for the Indus fan that controls the further expansion of Indus fan towards the west where Makran basin lies (Figs. 7 and 14). Maximum fan thickness reaches up to ~6.4 km downslope before confinement (Fig. 14). The thickness of the volcanic basement is roughly measured to be ~15 km as the total TWT reaches 12 s to the point where the first chaotic reflector of the basement is delineated. Towards the base of the fan, parallel beds are observed that are the assortment of lobes and cyclic deposits, capped by mega-turbidites and mass transport deposits (Fig. 14). The fan sediments are bisected with the maximum extension towards the east of the Murray ridge.

Maximum fan thickness on top of Murray ridge is observed to be ~1.6 km (Figs. 7 and 14). The maximum thickness of the fan in the study area peaks at 6.04 km west of the Murray ridge. West of the Murray ridge the entire extension of the fan is not surveyed.

5. Discussion

5.1. Channel levee growth

Subtle thickness variations and onlapping reflectors of the Indus fan suggest the presence of syn-depositional topographical features in the study area (Fig. 14). The age of the encountered structural highs and carbonate platforms are the Cretaceous and Paleocene, respectively (Carmichael et al., 2009b; Shahzad et al., 2018, 2019). The highs were formed due to extensive volcanic events while the Indian plate passed over a reunion hotspot following its separation from Madagascar and the Seychelles. These confinements are of the Paleocene to Eocene age that already developed before the initiation of the fan system. The low relief features acted as small basins that accommodated the sedimentation of the Indus fan (Figs. 14 and 15). The deposition of the Indus fan was highly influenced by the presence of the subsurface topography. Although the presence of these features is highlighted here, their areal extent cannot be deduced due to data limitations. The autogenic and allogenic controls have significantly influenced the distribution of fan deposits that developed the present geometry and architecture of the Indus fan.

This grain size partitioning as a result of confinements significantly affect the architecture of the basin deposits as the nature of the turbidity currents is modified downslope of the flow (Prather et al., 2006). The turbidites of the Indus fan suggest the deposition of coarser material because of trapped turbidity currents that could not flow further from the confinement that is also apparent from the presence of the smaller channels at the distal portion of the fan in the study area (Figs. 2 and 14). Thick beds of turbidites overlain on top of one another suggest the continuous deposition by turbidite deposits with thick columns of coarse material and an unconfined flow. High amplitude continuous reflections indicate that the turbidity currents were single sourced and carried large volumes of sediment (Harishidayat et al., 2018; henry w. posamentier and venkatarathnan kolla, 2003; Jobe et al., 2011). These deposits are overlain by continuous parallel to subparallel beds that thin towards the confinements and laterally continue draping the top of the confinement (Fig. 14).

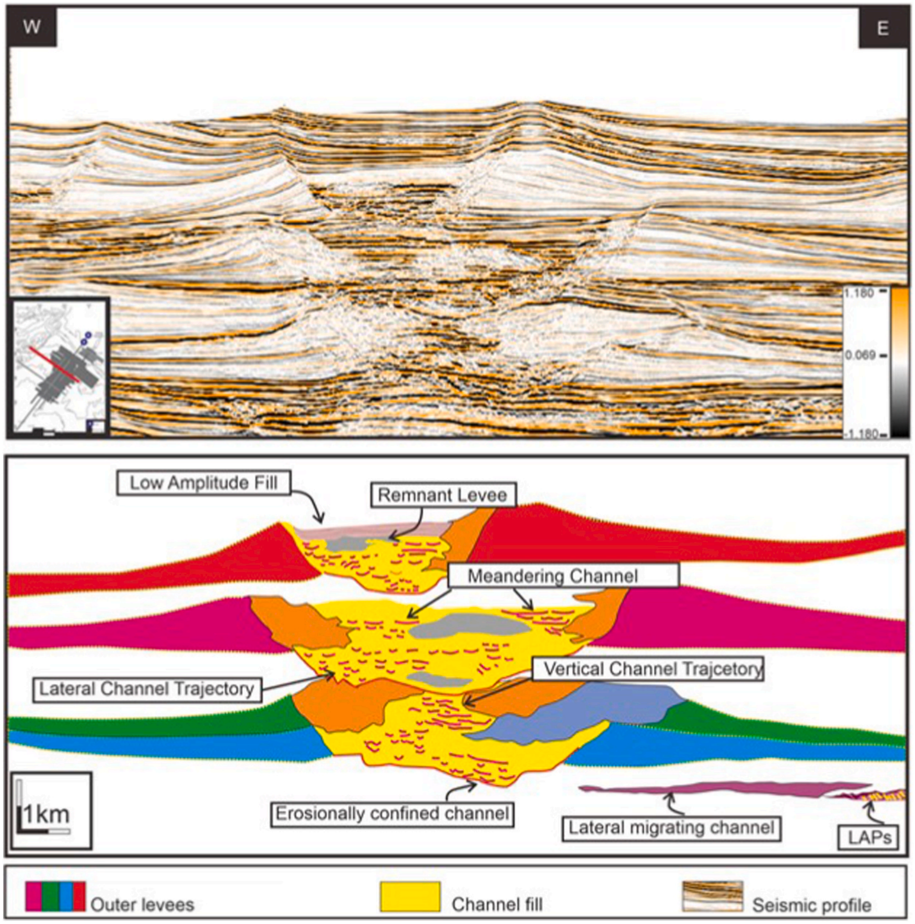

Fig. 9. Illustration of a channel complex set of Pliocene-Pleistocene age displaying the multiple incision to aggradation stage. Channel complexes display organized pattern of development undergoing varying channel migration trajectories. LAPs: Lateral Accretionary Packages. Color interpretation: Red, yellow, green, and blue fills represent levees; yellow fill with irregular lines represents channel fill; grey fill represents remnants of levees; brown fill represents the inner levees; pink color represents the bypass sediments overlaying the channel fill; purple color represents channel fill; Brown, black and white color reflections on uninterpreted seismic profile represent amplitude variations e.g., trough, crest, and zero-crossing polarity.

The structural influence on the channel complexes is also apparent, as the levees are asymmetric near the existing geomorphic features. This effect is not limited to tectonic structures but also due to preexisting channels levee complexes. The newly deposited levees follow the preexisting levees that often hamper the full growth and extent of either side of the levees.

Sediment waves are other prominent features that developed on the levee backslope during Plio-Pleistocene age (Table 2, facies 2 and Figs. 8 and 14). We suggest that these features develop because of flow stripping of fine-grained material from the turbidity currents and are deposited on the outer levees. Sediment waves also initiated due to underlying deformation structures developed on the outer levees. Sediment waves formed simultaneously during the formation of the channel. No deformation is visible on the sediment waves that may suggest the formation of sediment waves after the deposition of the outer levees. Sediment waves are rare to absent from Eocene-Oligocene to Miocene in the study area (Table 2**;** facies 2, 4, 7).

5.2. Lateral and unidirectional migration of channels

Lateral migration of channel and channel development as explained earlier (Figs. 9–11) is a consequence of three major steps that are involved in developing architecture of the channels. Firstly, sediment bypass takes places through channel incision that occurs on cyclic steps created by sediment waves on sea floor (Fildani et al., 2013), while the levee buildup initiates concurrently as the turbulent flow carries suspended particles (Eschard et al., 2003). Levee development in the proximal fan settings is reduced due to highly concentrated flows (Mulder and Alexander, 2001).

Secondly, upon the culmination of erosive processes and reduction in gravity flow, aggradation in the channel occurs as the channel abandonment phase establishes and a break in deposition occurs. This abandonment is followed by the initiation of phase three as the channel reactivates by the ensuing flows. Thirdly, onlaps and downlaps parallel to channel fill backstepping develop with the deposition of high amplitude reflections (HARs). Backstepping culminates with spill over lobes. Decreasing confinement and limited vertical growth (aggradation) of the channel result in the deposition of lateral high amplitude reflections. Volcanic basements significantly altered the lateral migration of the channels on the Indus fan (Fig. 14). Degree of confinement is subject to amount of lateral migration as abrupt and persistent lateral migrations greatly reduce degree of confinement, which is contrary to limited laterally migrating channel where confinement increases near the abandonment of the channel. Another impact of consistent lateral migration of the channel is that it erodes the levee deposited in the direction of the movement thus reflecting the apparent low confinement on one side of the channel whereas, the levees in the opposite direction prograde consistently towards the migration direction (Figs. 10–12).The results show that channel migration form zones of cut off and lateral accretionary packages with erosion on the inner side and deposition on the outer side of the channels. Outer bank of the migrating channel witness adjacent stacking of series of reflections in the direction of migration termed as Lateral Accretionary Packages (LAPs). High amplitude (orange) reflections spread on the time slice near the bends of the channel belts are LAPs which are produced by the lateral migration of the channel. Lateral accretionary packages (LAPs) are dipping reflections either parallel or dipping towards the channel associated with lateral migration of the channel (Abreu et al., 2003). LAPs are amalgamated to semi amalgamated depending on the flow energy, flow thickness and flow variations (Abreu et al., 2003). High amplitude

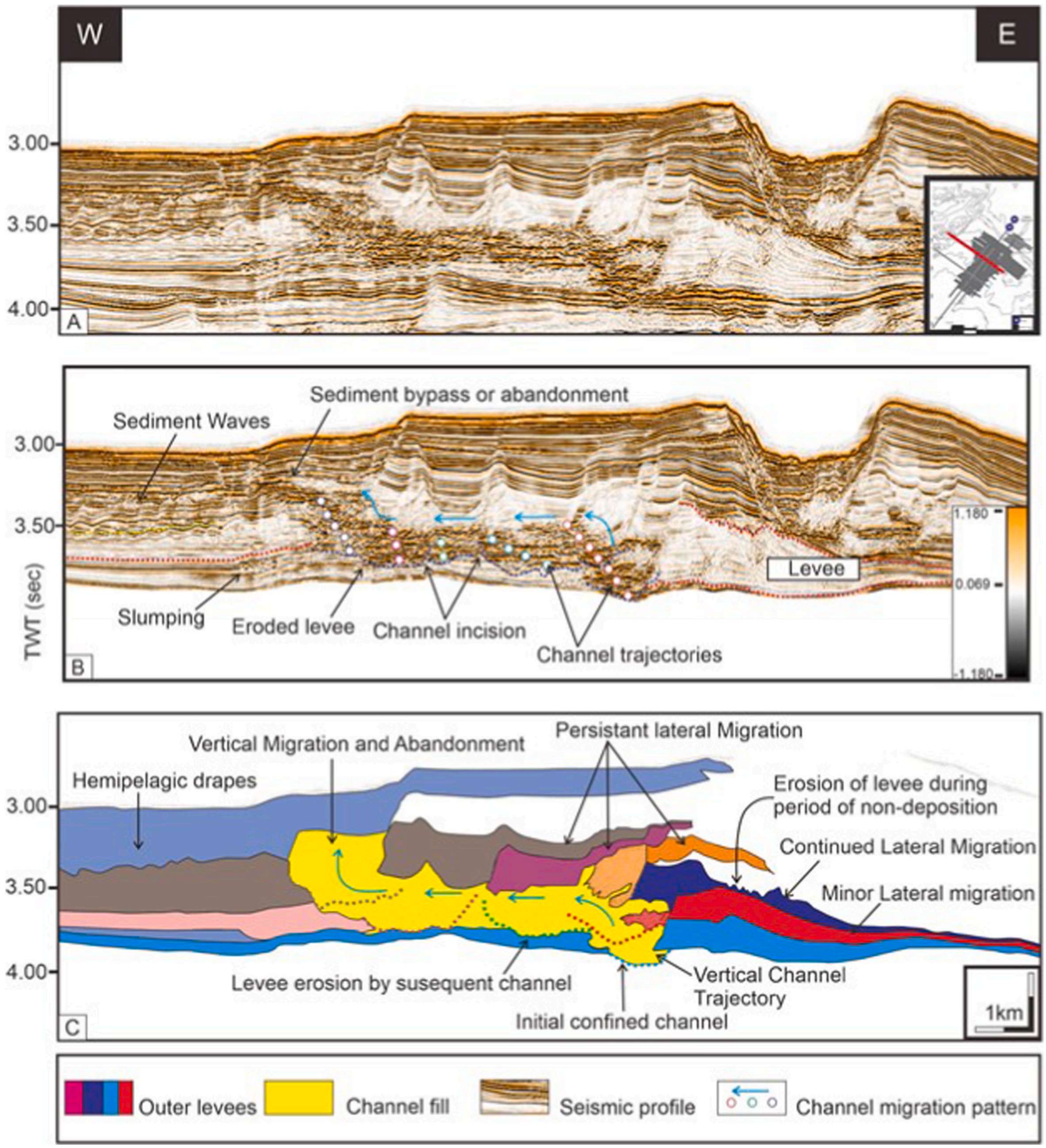

Fig. 10. A: Uninterpreted seismic profile of unidirectionally migrating major channels. channel. B: Channel trajectories indicate the growth pattern of the unidirectional laterally migrating channels. Successive turbidity currents migrated towards the outer bend of the channels in an organized pattern incising new channels followed by abandonments. Outer levee on the outer channel bank is eroded by the younger channels whereas a thick levee set is deposited on the inner bank that dips towards the thalweg. C: Multi-color fills showing the facies of laterally migrating channel. Sediment waves are deposited on the outer bend levee created by overspilling of turbidity currents. Color interpretation: blue arrows on profile "B" represent the channel migration; red dotted lines mark the outlines of levees; red dotted lines mark the basal erosive surface; white circles represent the channel fill trajectories; Blue fills on profile "C" represents the hemipelagic drapes; yellow fill with blue arrows represents the channel fill; grey, purple, blue, red, light blue, pink colors represent the outer levees. Dotted lines represent the basal erosive surface. Brown, black, and white color reflections on uninterpreted seismic profile represent the amplitude variations.

reflection packages observed on the seismic profile suggest that LAPs are a result of high energy and thick concentration turbidity flows. Shingled reflections or lateral accretionary packages are associated with the continuous lateral migration of the channel. They are deposited on the inner side of the channel with erosion on the outside margin of the channel belt. Lateral migration of the channel creates progradational inner levees with characteristic of parallel but low amplitude reflections (Figs. 10–12). Although lateral overflow deposits suggest that channel aggraded while migrating laterally (Eschard et al., 2003). If the ratio of amount of incision on the channel edges is smaller against aggradation ratio of the sediments within them, the shingled channel features or lateral accretionary packages will form (Deptuck et al., 2003). On the contrary if the ratio of incision is higher, no accumulation or aggradation will occur. Channel filling is far from random where entire channel complex reflects a systematic lateral migration while constituting a complex depositional architecture. It is also observed that long term incision and aggradation cycles tend to create complex depositional patterns that may show disorganized system (Sylvester et al., 2011). Neck cut off zones have high amplitudes which implies the lateral channel migration as well as the channel belt course adjustment,

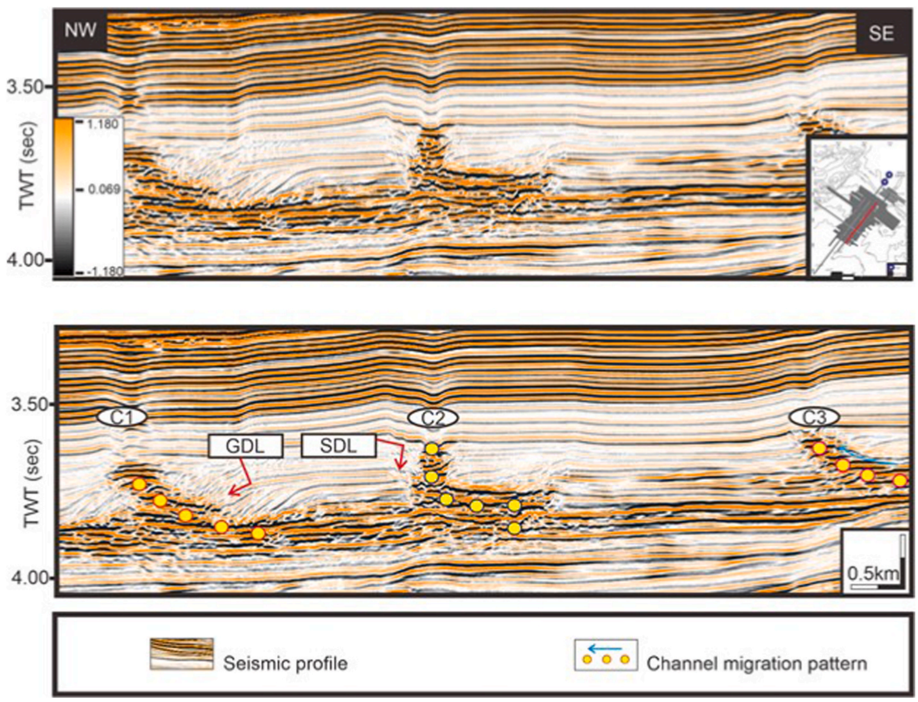

Fig. 11. Channel trajectories of unidirectionally migrating minor channels (UDMi) categorized as "C1", "C2", and "C3". UDMi channels do not undergo multiple stages of channel abandonment and reactivation stages, capped by concave down reflections. GDL: Gently Dipping Levee. SDL: Steeply Dipping Levee. Color interpretation: white circles represent the channel fill trajectories (growth patterns); Brown, black and white color reflections on uninterpreted seismic profile represent amplitude variation.

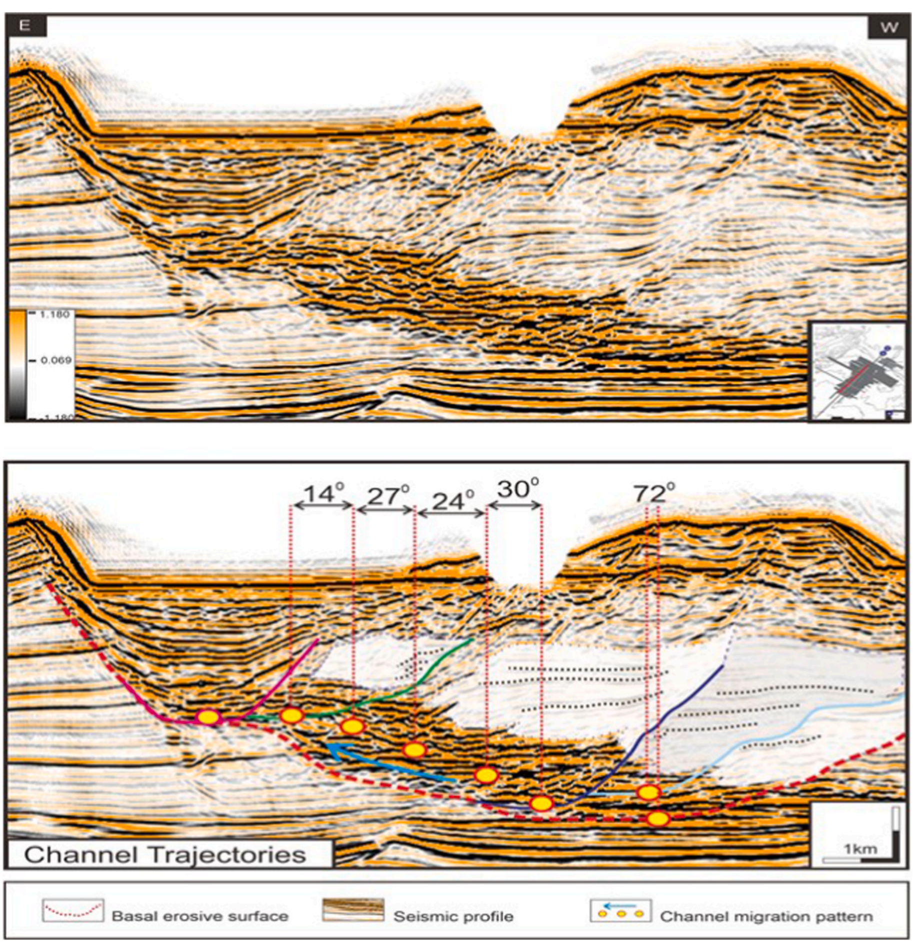

Fig. 12. A: Seismic profile with unidirectionally migrating channel. B: Angles of channel growth in unidirectionally migrating channels. Higher angles suggest the vertical growth and aggradation of channel fill. Smaller angles indicate the higher component of lateral migration of channel. Color interpretation: Brown, black and white color reflections on seismic profile represent the amplitude variations (polarity of data); red dotted line represents the basal erosive surface; white circles represent the channel fill trajectory. Angle reference: "0" degrees represent lateral migration of channels whereas "90" degrees represent aggradation of channel. Angles are calculated based on the migration pattern of the channels. Unfilled portion near sea floor marks the data muting and the inset image shows vertical scale.

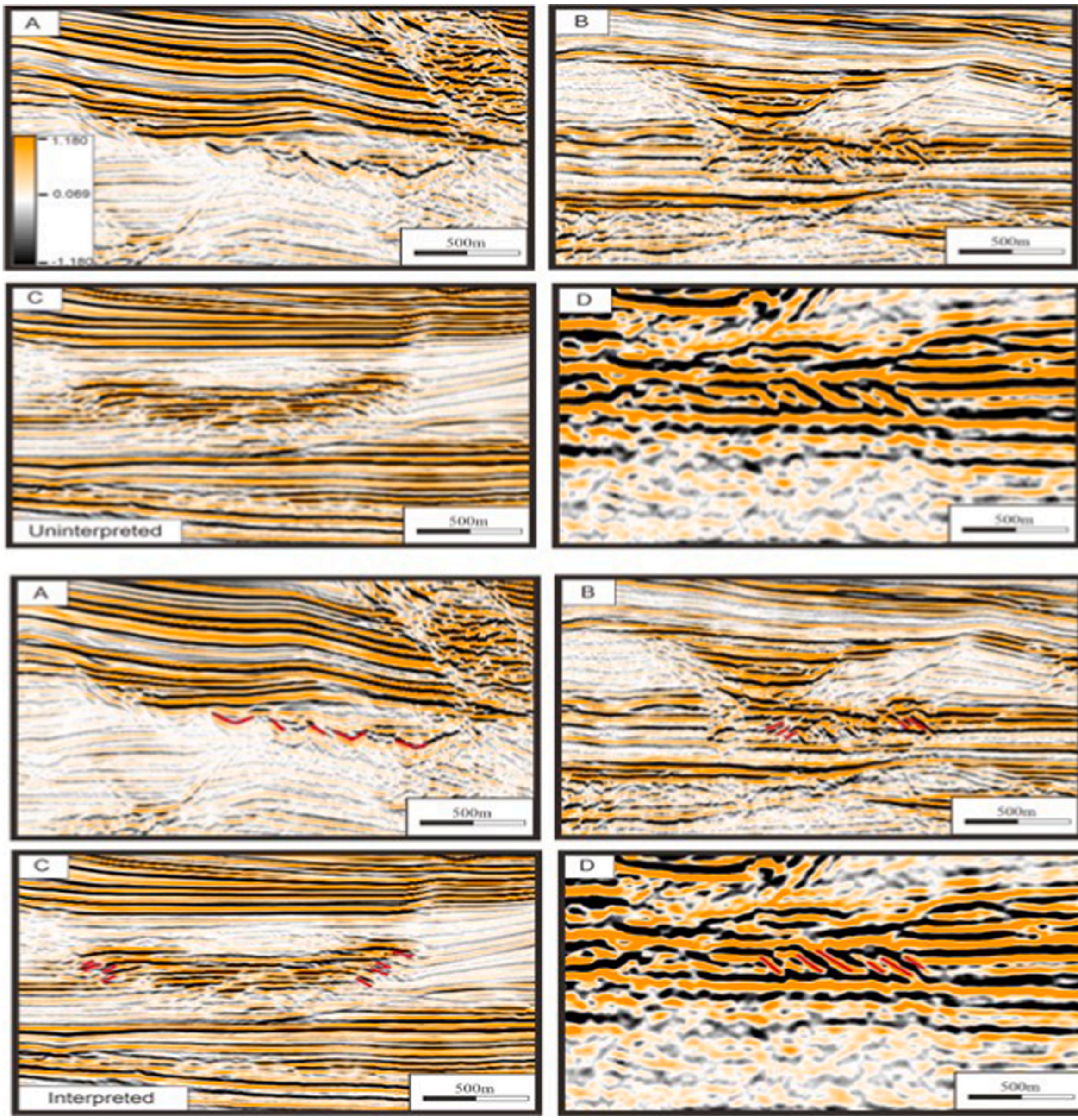

Fig. 13. Upper: Seismic profiles "A", "B", "C" and "D" show laterally migrating channels. Figures "A", "B", and "D" are unidirectionally migrating channels whereas figure "C" shows bi-directionally migrating channel with shift in migration direction as the channel developed. Lower: interpretation of lateral migration of channel characterized by lateral accretionary packages from distinct channel forms and sizes. Red oblique lines represent the lateral accretion packages created due to lateral migration of the channels. Color interpretation: Brown, black and white color reflections on seismic profile represent polarity of the data.

suggesting coarser depositions on the outer bank in submarine channel.

The sinuosity of the channel is subjected to the flow velocity and flow thickness (Kane et al., 2008; Peakall and Sumner, 2015). Channels in the early phase of the development on the Indus fan particularly in Pleistocene age are highly sinuous with low channel dimensions. These relatively small channels of the Plio-Pleistocene age channels have low degree of incision but significant unidirectional lateral migration with higher aggrading component (Fig. 11). This observation is in contrast to the elongated channels observed in glacial trough mouth fans (Bellwald et al., 2020).Smaller turbidity current developed the architecture of the channels and unlike the larger channels that have frequent cut and fill episodes these channels lack the reactivation post abandonment.

5.3. Allogenic and autogenic controls on sedimentation

The different channel morphologies are the result of varying sedimentation rates, climatic variations (most notably the South Asian monsoon), glaciation and sea level fluctuations, etc. Sea level fluctuations overtime significantly altered the active growth of the Indus fan that is apparent from the deposition of hemipelagic drapes and small-scale channel incisions (Figs. 2, 7, 8, 10 and 11). Plio-Pleistocene channels are draped by thick successions of hemipelagic drape (Figs. 2, 7 and 8). Orogeny of the Himalayas has caused higher levels of erosion thus higher sediments supply at the source (Curray, 1994). The thick turbidity flows with the tendency to carry coarser and thicker columns of sediments accrued architectural and morphological modifications. Most of the sediments carried by turbidity currents to the Indus fan are delivered by the Indus River that transports the sediments of five main rivers originating from the Himalayas and the Karakorum ranges.

The channel architecture is primarily modified by the influx of the sediments. The channel architecture of the Bengal fan (Hübscher et al., 1997) is similar to that of Indus fan in terms of complexity but the channel aspect ratios and dimensions vary as a consequence of sediment influx and probably due to the geometry of feeder canyon. In

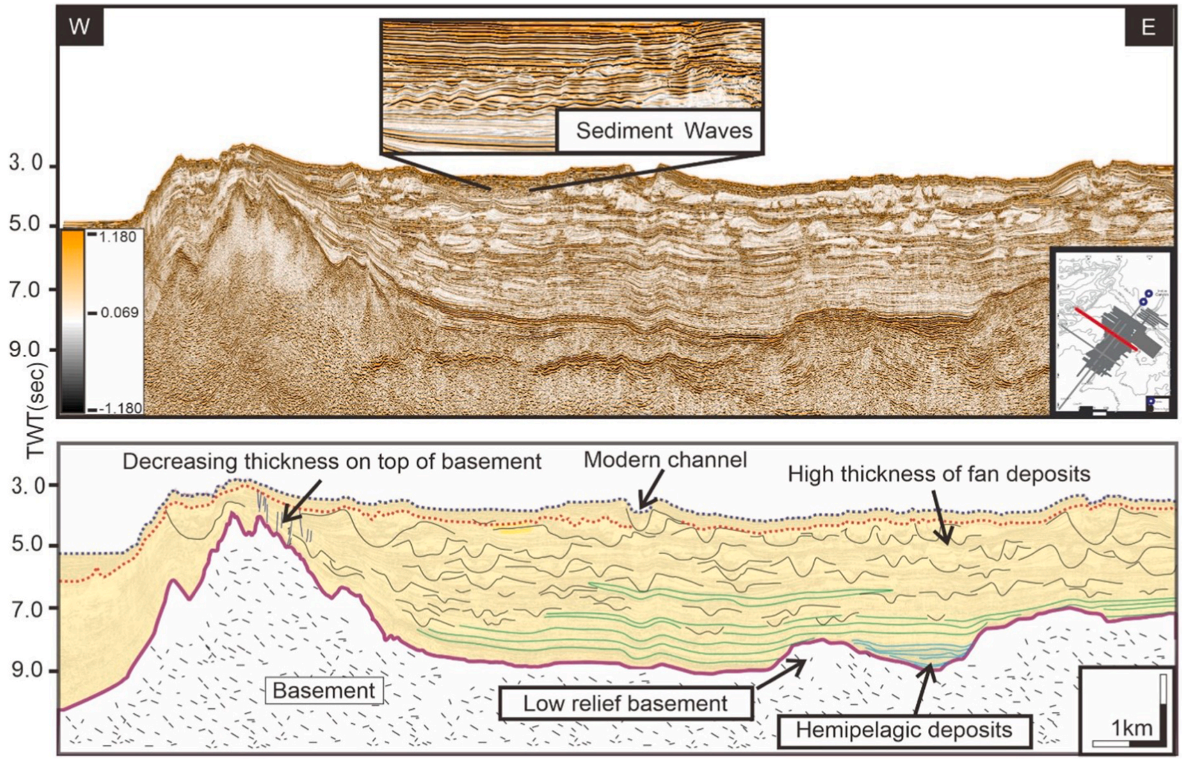

Fig. 14. Indus fan in the early stages of development is hindered in growth and lateral extension by the confinements created by volcanic basements colored in white. Following the healing phase Indus fan expanded laterally with an increasing supply of sediment that caused the progradation of the fan. High sediment influx and multiple stages of cut and fill created a complex channel architecture with high channel dimensions from the Eocene-Oligocene to the Plio-Pleistocene age. Color interpretation brown and white color reflections on seismic profile represent amplitude variations; off whit -light brown color fill represent the fan deposits; black wavy lines represent the basal erosive surfaces; blue solid line represents the base of hemipelagic deposits and blue dotted line represent the top of the Indus fan deposits. Green lines represent mass transport deposits; blue color vertical lines represent faults.

comparison with the Benin major channel levee system, the channel dimensions of Indus fan are staggeringly high. Benin major channel levee system maximum thickness reaches to 450 m (Deptuck et al., 2003) whereas our study suggest the maximum thickness of the channels reach up to 1200 m. The outer levees on Indus fan are much steeper that border a much deeper erosional fairway contrary to Benin major CLS on Niger delta. The different architecture of submarine fans globally points to the fact that sediment influx, canyon geometry and the processes acting near the sediment source highly influence the channel architecture.

The orogeny as a result of the Indian-Eurasian plate collision during the Eocene increased the sediment supply that was further aggravated as a result of extreme climatic conditions (Asian monsoons and glaciation) (Prins and Postma, 2000; Huyghe et al., 2001). Three major sources of sediments i.e., the Himalayan ranges, the Indus suture zone, and the Indian shield along with the Murray ridge stripping aided in building of the Paleogene Indus fan. Thick Paleogene turbidite clastic sediments have been in the Makran accretionary prism presumed to be deposited on the paleo-Indus fan, west of the modern Indus fan (DSDP site 221). Increasing mass wasting events and rich sediment carrying transporting agents dumped excess amounts of sediments in the Indus fan (Figs. 14 and 15). Paleogene Indus fan observed higher rates of mass wasting because of active tectonic regimes such as Indian-Arabian and Indian-Eurasian plate interaction and Early Miocene uplift of the Murray and Owen ridges.

Factors such as monsoon and tectonics in combination with sea level fluctuations meticulously controlled the development of |the Indus fan. Falling sea levels increased the rate of mass wasting whereas high stand conditions inhibited the transport of sediments downslope (Fig. 15). During rising sea level initial development of the fan occurred followed by a phase of mass wasting in the Miocene probably because of shelf exposure and extension of canyon downslope (Fig. 15). During Plio-Pleistocene progradation of the fan occurred and the sediment influx increased augmenting the complexity of channel architecture.

6. Conclusions

In the upper part of the Indus fan from the Pliocene to the Quaternary, we observed multiple cycles of incision to aggradation and higher channel abandonment to reactivation in comparison to the lower part from Eocene-Oligocene to Miocene age. Slope failure have caused the deposition of the mass transport deposits marking the inactive phase of turbidite deposition. Thick successions of megaturbidites on the top of volcanic basement also suggest the high sedimentation rate. However, a detailed investigation is required to understand the origin of these megaturbidites. Unidirectional migration of the channel increased from the Miocene to the Recent which is lacking or limited to the lower part of the Indus fan which is of the Eocene-Oligocene. Abrupt lateral migration is not encountered in the study area from the Eocene-Oligocene to Miocene whereas it has occurred excessively from Pliocene to Recent (Holocene). The Indus fan in its earlier stages of development from the Eocene-Oligocene to Miocene developed in constrained environments unlike during the later stages of fan development from Pliocene to Recent where no major morphological constraints hindered its growth. Sediment waves are abundantly present in the Pleistocene channels which suggest the occurrences of highly turbulent and thick sediment carrying turbidity flows. Our interpretation shows no sediment waves are encountered in the older successions from Eocene-Oligocene to Miocene.

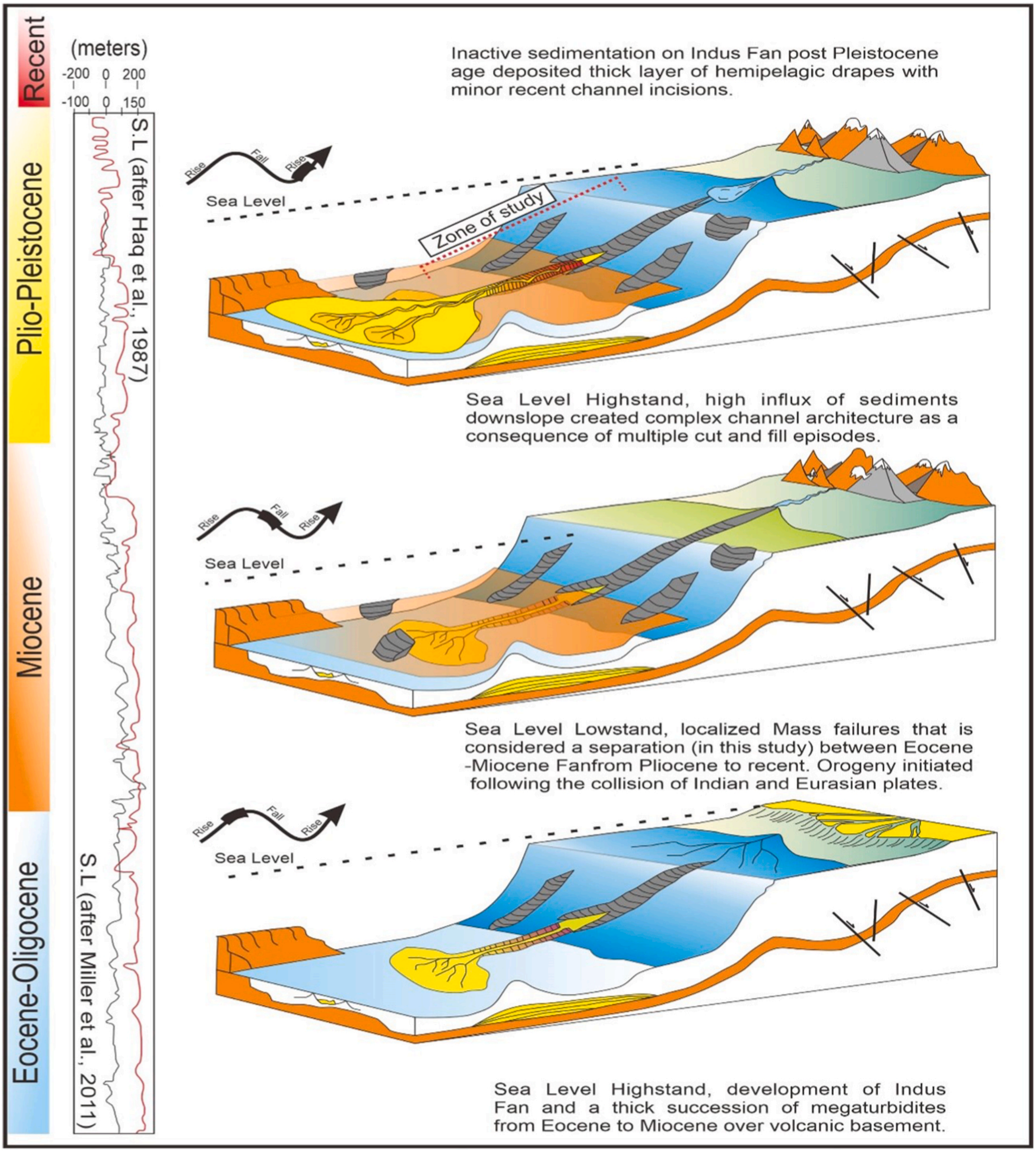

Fig. 15. Indus fan developed in multiple stages in congruence with the sea level fluctuation and tectonic activity. The unavailability of data hinders the understanding of monsoon activity and tectonic impacts on development of Indus fan. The early stage of fan development is characterized by confined development of Indus fan. Confinements are created by the volcanic basement deposited during the Indian plate drift over a reunion hotspot and carbonate platforms. The compartmentalization of sediments created by features like Murray ridge occurred with coarser sediments retained upstream of the confinements hence a restricted fan development occurred. During the lowstand conditions, the shelf exposed and ensuing the slope failure represented by the thick succession of MTDs overlaying the Eocene Oligocene succession of fan. Unconfined development of fan followed the sea level rise. Post Pleistocene active channel development ceased that is evident from the presence of thick succession of hemipelagic sediments that drape the Indus fan with minor channel incisions that indicate the possible development of channels during sea level high stand conditions.

Credit author statement

Ehsan ul Haq: Define the methodology and implemented through interpretation of data, contributed to the writing of initial draft. Ji Youliang: Supervised the writing of this manuscript and provided guidance to understand Architectural complexities and morphological variations of the Indus fan till the conclusion of the manuscript. Hadayat Ullah: Contributed to the writing and revised the manuscript. Khurram Shahzad: Contributed to the interpretation and to develop understanding about Indus fan and its elements and identification and investigation of the architectural elements. Nisar Ahmed: Revised the methodology and manuscript text, contributed to the writing, improved the language, and prepare the initial and revised version of manuscript for submission. Saad Ahmed: Revised the manuscript and contributed to the writing. Muhammad Zaheer: Revised the manuscript and contributed to the writing.

Declaration of competing interest

The authors declare that they have no known competing financial interests or personal relationships that could have appeared to influence the work reported in this paper.

Data availability

Data will be made available on request.

Acknowledgement

The authors would like to thank Directorate General of Petroleum Concession (DGPC), Ministry of Petroleum and Natural Resources, Pakistan for providing the seismic and well data. Schlumberger are thanked for providing licenses to their software Petrel and Kingdom, respectively. The Natural National Science Foundation of China Grant #: 41672098 is also acknowledged for the financial support for this study.

References

Abreu, V., Sullivan, M., Pirmez, C., Mohrig, D., 2003. Lateral accretion packages (LAPs): an important reservoir element in deep water sinuous channels. Mar. Petrol. Geol. 20, 631–648. https://doi.org/10.1016/j.marpetgeo.2003.08.003.

Ahmed, N., Ali, S.H., Ahmad, M., Khalid, P., Ahmad, B., Akram, M.S., Farooq, S., Din, Z. U., 2020. Subsurface structural investigation based on seismic data of the north-eastern Potwar basin, Pakistan. Indian J. Geo-Mar. Sci. 49 (7), 1258–1268.

Akram, N., Ahmed, N., Khan, M.S., Ehsan, M., Gul, M.A., Ahmad, M., 2020. Reservoir characterization by using petrophysical-electrofacies analyses and subsurface structural interpretation of the Nandpur gas field, middle Indus Basin, Pakistan. Himal. Geol. 41, 208–221.

Bellwald, B., Planke, S., Becker, L.W.M., Myklebust, R., 2020. Meltwater sediment transport as the dominating process in mid-latitude trough mouth fan formation. Nat. Commun. 11, 4645. https://doi.org/10.1038/s41467-020-18337-4.

Bourget, J., Zaragosi, S., Rodriguez, M., Fournier, M., Garlan, T., Chamot-Rooke, N., 2013. Late quaternary megaturbidites of the Indus fan: origin and stratigraphic significance. Mar. Geol. 336, 10–23. https://doi.org/10.1016/j.margeo.2012.11.011.

Brown, A.R., 2011. Interpretation of Three-Dimensional Seismic Data, Seventh. Society of Exploration Geophysicists and American Association of Petroleum Geologists. https://doi.org/10.1190/1.9781560802884.

Burbank, D.W., Beck, R.A., 1991. Models of aggradation versus progradation in the himalayan foreland. Geol. Rdsch. 80, 623–638. https://doi.org/10.1007/BF01803690.

Campion, K.M., Sprague, A.R., Mohrig, D., Lovell, R.W., Drzewiecki, P.A., Sullivan, M.D., Ardill, J.A., Jensen, G.N., Sickafoose, D.K., 2000. Outcrop Expression of Confined Channel Complexes 127–150.

Carmichael, S.M., Akhter, S., Bennett, J.K., Fatimi, M.A., Hosein, K., Jones, R.W., Longacre, M.B., Osborne, M.J., Tozer, R.S.J., 2009a. Geology and hydrocarbon potential of the offshore Indus Basin, Pakistan. Petrol. Geosci. 15, 107–116. https://doi.org/10.1144/1354-079309-826.

Carmichael, S.M., Akhter, S., Bennett, J.K., Fatimi, M.A., Hosein, K., Jones, R.W., Longacre, M.B., Osborne, M.J., Tozer, R.S.J., 2009b. Geology and hydrocarbon potential of the offshore Indus Basin, Pakistan. Petrol. Geosci. 15, 107–116.

Clift, P., Gaedicke, C., 2002. Accelerated mass flux to the Arabian Sea during the middle to late Miocene. Geol. 30, 207. https://doi.org/10.1130/0091-7613(2002)030<0207:AMFTTA>2.0.CO, 2.

Clift, P.D., Shimizu, N., Layne, G.D., Blusztajn, J.S., Gaedicke, C., Schlüter, H.-U., Clark, M.K., Amjad, S., 2001. Development of the Indus fan and its significance for the erosional history of the western himalaya and karakoram. Geol. Soc. Am. Bull. 113, 1039–1051. https://doi.org/10.1130/0016-7606(2001)113<1039:DOTIFA>2.0.CO, 2.

Clift, Peter, Gaedicke, Christoph, Edwards, Rosemary, Lee, Jae Il, Hildebrand, Peter, Amjad, Shahid, Robert, S., White, Schlüter, Hans-Ulrich, 2002. The stratigraphic evolution of the Indus Fan and the history of sedimentation in the Arabian Sea. Mar. Geophys. Res. 223–245. https://doi.org/10.1023/A:1023627123093.

Curray, J.R., 1994. Sediment volume and mass beneath the bay of bengal. Earth Planet Sci. Lett. 125, 371–383. https://doi.org/10.1016/0012-821X(94)90227-5.

Damuth, J.E., Flood, R.D., 1985. Amazon Fan, Atlantic Ocean. In: Bouma, A.H., Normark, W.R., Barnes, N.E. (Eds.), Submarine Fans and Related Turbidite Systems. Springer New York, New York, NY, pp. 97–106. https://doi.org/10.1007/978-1-4612-5114-9_15.

Damuth, J.E., Flood, R.D., Kowsmann, R.O., Belderson, R.H., Gorini, M.A., 1988. Anatomy and Growth Pattern of Amazon Deep-Sea Fan as Revealed by Long-Range Side-Scan Sonar (GLORIA) and High-Resolution Seismic Studies. AAPG Bull. (United States).

Deptuck, M.E., Steffens, G.S., Barton, M., Pirmez, C., 2003. Architecture and evolution of upper fan channel-belts on the Niger Delta slope and in the Arabian Sea. Mar. Petrol. Geol. 20, 649–676. https://doi.org/10.1016/j.marpetgeo.2003.01.004.

Ehsan, M.I., Ahmed, N., Khalid, P., Wei, L.X., Naeem, N., 2016. An application of rock physics modeling to quantify the seismic response of gas hydrate-bearing sediments in Makran accretionary prism, offshore, Pakistan. Geosci. J. 20, 321–330.

Emmel, F.J., Curry, J.R., 1981. Channel piracy on the lower bengal fan. Geo Mar. Lett. 1, 123–127.

Eschard, R., Albouy, E., Deschamps, R., Euzen, T., Ayub, A., 2003. Downstream evolution of turbiditic channel complexes in the Pab Range outcrops (Maastrichtian, Pakistan). Mar. Petrol. Geol. 20, 691–710. https://doi.org/10.1016/j.marpetgeo.2003.02.004.

Fildani, A., Hubbard, S.M., Covault, J.A., Maier, K.L., Romans, B.W., Traer, M., Rowland, J.C., 2013. Erosion at inception of deep-sea channels. Mar. Petrol. Geol. 41, 48–61. https://doi.org/10.1016/j.marpetgeo.2012.03.006.

Flood, R.D., Manley, P.L., Kowsmann, R.O., Appi, C.J., Pirmez, C., 1991. Seismic Facies and Late Quaternary Growth of Amazon Submarine Fan. In: Weimer, P., Link, M.H. (Eds.), Seismic Facies and Sedimentary Processes of Submarine Fans and Turbidite Systems. Springer New York, New York, NY, pp. 415–433.

Gaedicke, C., Schlüter, H.-U., Roeser, H.A., Prexl, A., Schreckenberger, B., Meyer, H., Reichert, C., Clift, P., Amjad, S., 2002. Origin of the northern Indus fan and Murray Ridge, northern Arabian sea: interpretation from seismic and magnetic imaging. Tectonophysics 355, 127–143. https://doi.org/10.1016/S0040-1951(02)00137-3.

Gardner, M.H., Borer, J.M., Melick, J.J., Mavilla, N., Dechesne, M., Wagerle, R.N., 2003. Stratigraphic process-response model for submarine channels and related features from studies of Permian Brushy Canyon outcrops, West Texas. Mar. Petrol. Geol. 20, 757–787. https://doi.org/10.1016/j.marpetgeo.2003.07.004.

Gee, M.J.R., Gawthorpe, R.L., Bakke, K., Friedmann, S.J., 2007. Seismic geomorphology and evolution of submarine channels from the Angolan continental margin. J. Sediment. Res. 77, 433–446. https://doi.org/10.2110/jsr.2007.042.

Ghazi, S., Ali, S.H., Shahzad, T., Ahmed, N., Perveiz, K., Akram, S., Ali, S., Sami, J., 2020. Sedimentary, structural and salt tectonic evolution of Karoli-Nilawahan area, central salt range and its impact for the potwar province. Himal. Geol. 41, 145–156.

Gombos, A.M., Powell, W.G., Norton, I.O., 1995. The tectonic evolution of western India and its impact on hydrocarbon occurrences: an overview. Sediment. Geol. 96, 119–129. https://doi.org/10.1016/0037-0738(94)00129-I.

Harishidayat, D., Omosanya, K.O., Johansen, S.E., Eruteya, O.E., Niyazi, Y., 2018. Morphometric analysis of sediment conduits on a bathymetric high: implications for palaeoenvironment and hydrocarbon prospectivity. Basin Res. 30, 1015–1041. https://doi.org/10.1111/bre.12291.

Hodgson, D.M., Di Celma, C.N., Brunt, R.L., Flint, S.S., 2011. Submarine slope degradation and aggradation and the stratigraphic evolution of channel–levee systems. J. Geol. Soc. 168, 625–628. https://doi.org/10.1144/0016-76492010-177.

Hübscher, C., Spieβ, V., Breitzke, M., Weber, M.E., 1997. The youngest channel-levee system of the Bengal Fan: results from digital sediment echosounder data. Mar. Geol. 141, 125–145. https://doi.org/10.1016/S0025-3227(97)00066-2.

Hussain, M., Ahmed, N., 2018. Reservoir geomechanics parameters estimation using well logs and seismic reflection data: insight from Sinjhoro Field, Lower Indus Basin, Pakistan. Arabian J. Sci. Eng. 43, 3699–3715.

Hussain, M., Chun, W.Y., Khalid, P., Ahmed, N., Mahmood, A., 2017. Improving petrophysical analysis and rock physics parameters estimation through statistical analysis of Basal sands, lower Indus basin, Pakistan. Arabian J. Sci. Eng. 42, 327–337.

Huyghe, P., Galy, A., Mugnier, J.-L., France-Lanord, C., 2001. Propagation of the thrust system and erosion in the Lesser Himalaya: geoch. sediment. evidence. Geol. 29, 1007. https://doi.org/10.1130/0091-7613(2001)029<1007:POTTSA>2.0.CO, 2.

Jobe, Z.R., Lowe, D.R., Uchytil, S.J., 2011. Two fundamentally different types of submarine canyons along the continental margin of Equatorial Guinea. Mar. Petrol. Geol. 28, 843–860. https://doi.org/10.1016/j.marpetgeo.2010.07.012.

Kane, I.A., McCaffrey, W.D., Peakall, J., 2008. Controls on sinuosity evolution within submarine channels. Geology 36, 287. https://doi.org/10.1130/G24588A.1.

Kenyon, N.H., Amir, A., Cramp, A., 1995. Geometry of the Younger Sediment Bodies of the Indus Fan. In: Pickering, K.T., Hiscott, R.N., Kenyon, N.H., Ricci Lucchi, F., Smith, R.D.A. (Eds.), Atlas of Deep Water Environments. Springer Netherlands, Dordrecht, pp. 89–93. https://doi.org/10.1007/978-94-011-1234-5_16.

Kolla, V., Coumes, F., 1983. Morpho-acoustic and sedimentologic characteristics of the Indus fan. Geo Mar. Lett. 3, 133–139. https://doi.org/10.1007/BF02462458.

Kolla, V., Coumes, F., 1985. Indus Fan, Indian Ocean. In: Bouma, A.H., Normark, W.R., Barnes, N.E. (Eds.), Submarine Fans and Related Turbidite Systems. Springer New York, New York, NY, pp. 129–136. https://doi.org/10.1007/978-1-4612-5114-9_19.

Kolla, V., Macurda Jr., D.B., 1988. Sea-level changes and timing of turbidity-current events in deep-sea fan systems. https://doi.org/10.2110/pec.88.01.0381.

Mayall, M., Jones, E., Casey, M., 2006. Turbidite channel reservoirs—key elements in facies prediction and effective development. Mar. Petrol. Geol. 23, 821–841. https://doi.org/10.1016/j.marpetgeo.2006.08.001.

McHargue, T.R., 1991. Seismic Facies, Processes, and Evolution of Miocene Inner Fan Channels, Indus Submarine Fan. In: Weimer, P., Link, M.H. (Eds.), Seismic Facies and Sedimentary Processes of Submarine Fans and Turbidite Systems. Springer New York, New York, NY, pp. 403–413. https://doi.org/10.1007/978-1-4684-8276-8_22.

McHargue, T.R., Webb, J.E., 1986. Internal geometry, seismic facies, and petroleum potential of canyons and inner fan channels of the Indus submarine fan. Am. Assoc. Petrol. Geol. Bull. 70 (2), 161–180.

Metivier, Gaudemer, 1999. Stability of output fluxes of large rivers in South and East Asia during the last 2 million years: implications on floodplain processes. Basin Res. 11, 293–303. https://doi.org/10.1046/j.1365-2117.1999.00101.x.

Mitchum-jr, R.M., Vail, P.R., Thompson, S., 1977. Seismic stratigraphy and global changes of sea level, Part 2: the depositional sequence as a basic unit for stratigraphic analysis. AAPG mem 26, 53–62.

Mulder, T., Alexander, J., 2001. The physical character of subaqueous sedimentary density flows and their deposits. Sedimentology 48, 269–299. https://doi.org/10.1046/j.1365-3091.2001.00360.x.

Mutti, E., Normark, W.R., 1987. Comparing Examples of Modern and Ancient Turbidite Systems: Problems and Concepts. In: Leggett, J.K., Zuffa, G.G. (Eds.), Marine Clastic Sedimentology. Springer Netherlands, Dordrecht, pp. 1–38. https://doi.org/10.1007/978-94-009-3241-8_1.

Naini, B.R., Kolla, V., 1982. Acoustic character and thickness of sediments of the Indus Fan and the continental margin of western India. Mar. Geol. 47, 181–195. https://doi.org/10.1016/0025-3227(82)90068-8.

Normark, W.R., 1978. Fan valleys, channels, and depositional lobes on modern submarine fans: characters for recognition of sandy turbidite environments. Am. Assoc. Petrol. Geol. Bull. 62, 912–931.

Normark, W.R., Hess, G.R., Stow, D.A.V., Bowen, A.J., 1980. Sediment waves on the monterey fan levee: a preliminary physical interpretation. Mar. Geol. 37, 1–18. https://doi.org/10.1016/0025-3227(80)90009-2.

Peakall, J., Sumner, E.J., 2015. Submarine channel flow processes and deposits: a process-product perspective. Geomorphology 244, 95–120. https://doi.org/10.1016/j.geomorph.2015.03.005.

Piper, D., Deptuck, M., 1997. Fine-grained turbidites of the Amazon fan: facies characterization and interpretation. In: https://doi.org/10.2973/odp.proc.sr.155.208.1997.

Posamentier, W.H., Venkatarathnan, K., 2003. Seismic geomorphology and stratigraphy of depositional elements in deep-water settings. J. Sediment. Res. 73, 367–388.

Prather, B., Pirmez, C., O'Byrne, C., D Winker, C., Mallarino, G., Droxler, A., B Flemings, P., Behrmann, C., John, C., 2006. Expedition 308 shipboard scientific party, I. In: Stratigraphic evolution of linked basins within the Brazos-Trinity slope system: western Gulf of Mexico, 308, pp. 101–108.

Prins, M.A., 1999. Pelagic, Hemipelagic and Turbidite Deposition in the Arabian Sea during the Late Quaternary: Unravelling the Signals of Eolian and Fluvial Sediment Supply as Functions of Tectonics, Sea-Level and Climate Change by Means of End-Member Modelling of Siliciclastic Grain-Size Distributions. Geologica Ultraiectina. Univ, Utrecht.

Prins, M.A., Postma, G., 2000. Effects of climate, sea level, and tectonics unraveled for last deglaciation turbidite records of the Arabian Sea. Geology 28, 375. https://doi.org/10.1130/0091-7613(2000)28<375:EOCSLA>2.0.CO, 2.

Rad, U.V., Tahir, M., 1997. Late Quaternary sedimentation on the outer Indus shelf and slope (Pakistan): evidence from high-resolution seismic data and coring. Mar. Geol. 138, 193–236. https://doi.org/10.1016/S0025-3227(96)00090-4.

Schwenk, T., Spiess, V., 2009. Architecture and Stratigraphy of the Bengal Fan as Response to Tectonic and Climate Revealed from High-Resolution Seismic Data. In: External Controls on Deep-Water Depositional Systems, pp. 107–131. https://doi.org/10.2110/sepmsp.092.107.

Shahzad, K., Betzler, C., Ahmed, N., Qayyum, F., Spezzaferri, S., Qadir, A., 2018. Growth and demise of a Paleogene isolated carbonate platform of the Offshore Indus Basin, Pakistan: effects of regional and local controlling factors. Int. J. Earth Sci. 107, 481–504. https://doi.org/10.1007/s00531-017-1504-7.

Shahzad, K., Betzler, C., Qayyum, F., 2019. Controls on the Paleogene carbonate platform growth under greenhouse climate conditions (Offshore Indus Basin). Mar. Petrol. Geol. 101, 519–539. https://doi.org/10.1016/j.marpetgeo.2018.12.025.

Sylvester, Z., Pirmez, C., Cantelli, A., 2011. A model of submarine channel-levee evolution based on channel trajectories: implications for stratigraphic architecture. Mar. Petrol. Geol. 28, 716–727. https://doi.org/10.1016/j.marpetgeo.2010.05.012.

Vail, P.R., Mitchum Jr., R.M., Thompson III, S., 1977. Seismic Stratigraphy and Global Changes of Sea Level, Part 4: Global Cycles of Relative Changes of Sea Level, vol. 26. https://doi.org/10.1306/M26490C6.